İSTANBUL TECHNICAL UNIVERSITY★EURASIA INSTITUTE OF EARTH SCIENCES

GEODYNAMIC MODELING THE STYLES OF LITHOSPHERIC DELAMINATION WITH APPLICATION TO THE EASTERN ANATOLIA

M.Sc. THESIS

Ö. Caner MEMİŞ

Department of Solid Earth Sciences

Geodynamics Programme

Thesis Advisor: Assoc. Prof. Dr. Oğuz Hakan GÖĞÜŞ

AUGUST 2016

İSTANBUL TECHNICAL UNIVERSITY★EURASIA INSTITUTE OF EARTH SCIENCES

GEODYNAMIC MODELING THE STYLES OF LITHOSPHERIC DELAMINATION WITH APPLICATION TO THE EASTERN ANATOLIA

M.Sc. THESIS

Ö. Caner MEMİŞ

Department of Solid Earth Sciences

Geodynamics Programme

Thesis Advisor: Assoc. Prof. Dr. Oğuz Hakan GÖĞÜŞ

AUGUST 2016

İSTANBUL TEKNİK ÜNİVERSİTESİ★AVRASYA YER BİLİMLERİ ENSTİTÜSÜ

LİTOSFERİK DELAMİNASYONUN DOĞU ANADOLU BÖLGESİ İÇİN JEODİNAMİK OLARAK MODELLENMESİ

YÜKSEK LİSANS TEZİ

Ö. Caner MEMİŞ
602131001

Katı Yer Bilimleri

Jeodinamik Programı

Tez Danışmanı: Doç. Dr. Oğuz Hakan GÖĞÜŞ

AĞUSTOS 2016

Caner Memiş, a M.Sc./ student of İTU Graduate School of Science Engineering and Technology student ID 602131001, successfully defended the thesis/dissertation entitled "GEODYNAMIC MODELING THE STYLES OF LITHOSPHERIC DELAMINATION WITH APPLICATION TO THE EASTERN ANATOLIA", which he/she prepared after fulfilling the requirements specified in the associated legislations, before the jury whose signatures are below.

Thesis Advisor : **Assoc. Prof. Dr. Oğuz Hakan GÖĞÜŞ**

Jury Members : **Prof. Dr. Mehmet Keskin**
İstanbul University

Prof. Dr. Russel Pysklywec
Toronto University

Assoc. Prof. Oğuz Hakan GÖĞÜŞ
İstanbul Technical University

Date of Submission :
Date of Defense :

TABLE OF CONTENTS

Page

LIST OF TABLES

Page

LIST OF FIGURES

Page

GEODYNAMIC MODELING THE STYLES OF LITHOSPHERIC DELAMINATION WITH APPLICATION TO THE EASTERN ANATOLIA

SUMMARY

The East Anatolia High Plateau is a young and active collision zone and also known as a part of Alp-Himalaya orogenesis belt. The east Anatolian High Plateau has been rised by the continental collision of the Arabian plate to the south towards Eurasian plate to the north. by continental collision (13 ma). Former studies suggest that during the convergence motion of Arabian plate; the lithosphere shortened and thickened beneath the East Anatolia and regional topography isostatically compensated by its thick lithosphere. However; recent deep geophysical studies show that regional topography being compensated by hot and convective asthenosphere instead of thick lithosphere and the most of plateau devoid of its mantle lithosphere. Petrological studies address that the first volcanic products in Erzurum-Kars plateau (13ma) characterized by an asthenospheric origin. Corroborating geophysical and geophysical findings, the geodynamic evolution of the plateau accounted by hypothesis of slab steepening and following break-off. According to this hypothesis; being subducted Neotethys's oceanic mantle lithosphere benath the Eastern Pontides has been decoupled from overlying accreted prism and afterward its broke-off. This hypothesis occurs similar to delamination theory which is introduced by Peter Bird (1979) for uplift of Colorado Plateau. In this work, by using 2D numerical modeling method, we test lithospheric delamination model by changing rheological, physical and mechanical parameters. Also, we investigated the effects of lower crustal rheology, mantle lithosphere plastic yield stress, mantle lithosphere density, plate convergence rate and crustal thickness on delamination processes. Model results show that the evolution of lithospheric delamination is optimum when the lower crustal rheology selected as felsic granulite. On the other hand, break-off event occurs dependent on mantle lithosphere plastic yield stress and plate convergence rate. The break-off events occurs earlier when the mantle lithosphere plastic yield stress value kept low (<75 MPa) compare to models in which used higher mantle lithosphere plastic yield stress. Furthermore, increasing plate convergence rates has a big role on rising of topography and thickening of crust, however; it has a negative effect on slab break-off. We were not observed break-off event at higher plate convergence rates (>2 cm/yr). The model results reconciled against observations in the eastern Anatolia and by selecting the most viable models we argued that conformity of the proposed model for regional geodynamic evolution.

Key Words: East Anatolian High Plateau, Delamination, Slab Break-off, Geodynamics

LİTOSFERİK DELAMİNASYONUN DOĞU ANADOLU BÖLGESİ İÇİN JEODİNAMİK OLARAK MODELLENMESİ

ÖZET

Doğu Anadolu Yüksek Platosu, Alp- Himalaya orojenez kuşağının bir parçası olup, günümüzde hala genç ve aktif olan kıtasal bir çarpışma bölgesidir. Güneyde Arap plakası kuzeyde Avrasya plakasının birbirleri ile çarpışması (13 Ma) sonucu yükselmiştir ve bugün deniz seviyesinden 2 km yükseklikte durmaktadır. Daha önce yapılan çalışmalar, Doğu Anadolu Yüksek Platosu' nun altında bulunan litosferin, çarpışmanın sonucu olarak kısaldığı ve kalınlaştığını, Plato' nun yüksek topoğrafyasının bu kalın litosfer tabakası ile izoztatik denge halinde olduğunu öne sürmekteydi. Ancak yapılan derin jeofizik gözlemler Doğu Anadolu Yüksek Platosu' nun altında bir manto litosferinin olmadığını göstermiş, bunun üzerinede bölge topoğrafyasının Doğu Anadolu' nun altından kopan manto litosferi parçasının yerine yükselen, sıcak ve konvektif olan astenosfer ile dinamik olarak dengede olduğu yorumu getirilmiştir. Petrolojik çalışmalar da 13 My. Önce, Erzurum-Kars platosu' nda başlayan volkanizmanın astenosfer kökenli olduğunu göstermektedir. Jeofizik ve jeolojik bulgular yardımı ile platonun yükselme mekanizması dalan levhanın dikleşmesi ve ardından kopması hipotezi ile açıklanmaktadır. Bu hipoteze gore; güneyde Arap ve Avrasya kıtaları arasında bulunan Neo-Tetis okyanusu' nun güney kolunun kapanması sırasında Bitlis-Pötürge Massifi' ne ait okyanusal litosfer, kendisini üzerlemekte olan yığışım prizmasından dikleşerek kopmuştur. Bu hipotez, 1979' da Peter Bird tarafından Kolorado Platosu' nun yükselmesi için önerilmiş olan 'delaminasyon' hipotezi ile benzer şekilde tezahür etmektedir. Bu çalışmada; iki boyutlu sayısal modelleme yardımı ile yeriçi reolojik, fiziksel ve mekanik parametreleri değiştirilip litosfer delaminasyonu ve kopması modelleri Doğu Anadolu Platosu' nun jeodinamik evriminin daha iyi anlaşılması amacı ile test edilmiştir. Ayrıca alt kabuk reolojisi, manto litosferi plastik yenilme değeri, manto litosferi yoğunluğu, levha hızı, ve kabuk kalınlığı gibi parametrelerin litosfer delaminasyonunun evrimi üzerindeki etkileri ortaya konumuştur. Model sonuçları, delaminasyon evriminin felsik granulit reolojide alt kabuk kullanığında optimum olduğunu göstermektedir. Levha kopması ise manto litosferi plastik yenilme değerine ve levha hızına bağlı olarak gerçekleşmektedir. Manto litosferi plastik yenilme değeri düşük tutulduğunda (<75 MPa) levhanın kopması yüksek plastisite değeri kullanılan modellere göre daha erken tezahür etmektedir. Artan levha hızı ise dalan levhanın kopması üzerinde negatif bir etki yaratırken >2cm/yıl dan büyük hızlarda levha kopması gözlenmemiştir, topoğrafya ve kabuk kalığınlığının artamasında önemli bir role sahiptir. Modellerden elde sonuçları ile Doğu Anadolu' nun gözlenebilir verilerinin karşılaştırılması sayesinde, platonun jeodinamik evrimini en uygun karışılayan modeller seçilip önerilen hipotezin bölge jeodinamiğini açıklama kabiliyeti tartışılmıştır.

Anahtar Kelimeler: Doğu Anadolu Yüksek Platosu, Delaminasyon, Levha kırılması, Jeodinamik

1. FUNDAMENTALS

1.1 Lithosphere

The term of lithosphere describes the rigid outer layer of the Earth (Figure 1.1). Lithosphere is not in homogenous nature and shows the physical, chemical varieties therefore rheological differences occur mainly based on its containing rocks and change in temperature with depth (geotherm). This is because the appearing of the boundary layers, which are detected by indirect geophysical surveys and it associated with distinct variations in rheology. Lithosphere can extend depth of around 300 km and comprises the crust and non-convecting uppermost mantle called mantle lithosphere. The lithosphere lies on top of the asthenosphere and the temperature of the lithosphere asthenosphere boundry is around 1350 C. We know the constitution of upper mantle and available boundaries from seismic constraints (mantle P wave velocity ~8 km/sec). The obtained seismic data also help us to infer that densities of Earth interior rocks using by principle of acoustic impedance, since the seismic waves travel as a function of density of the rocks as directly proportionally. For example, seismic speed of 8 km/sec corresponds to density of about 3.2 /cm3(etc peridotite, eclogite). Namely, the calculation of seismic wave speeds by using empirical formulations give us the information of the rigid part of the Earth.

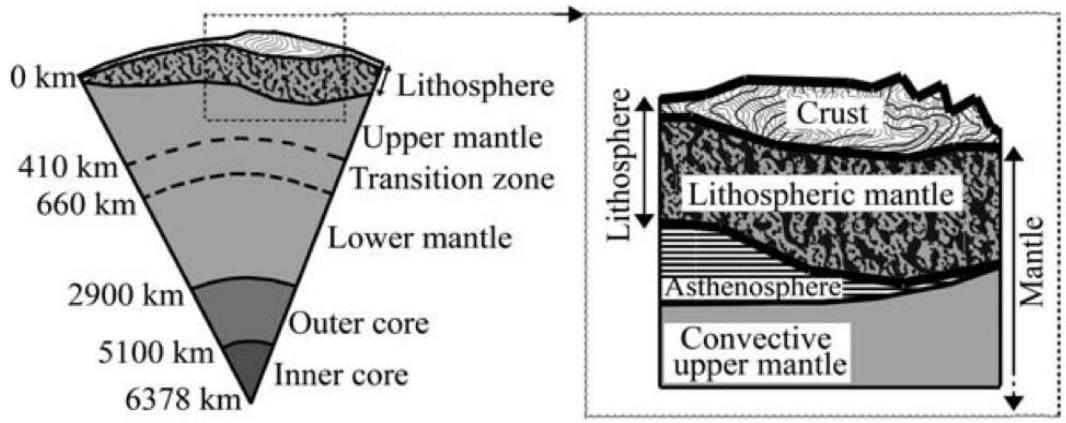

Figure 1.1 : The Earth's inside layers and the structure of lithosphere (Artemieva, 2011).

1.2 How the Lithosphere Forms?

The history of lithospheric plates has been commenced by Alfred Wegener (1880-1930). He was the first person who asking questions on puzzle-like edged continents, concurrently evolved lizards in different transoceanic continents. Terminally, he introduced the Pangea. Today we know the Pangea as the name of the supercontinent that was existed before brake up of Pangea into continents. Wegener called the theory as continental drift (Wegener, 1966). By the means of the theory of continental drift, a number of geological events explained excepting that why the continents moved. When became to 1960's, a geologist who Harry Hess proposed the seafloor spreading (Hess, 1962). It was a concept in which the new oceanic lithosphere forms. Subsequently, the mobile lithosphere concept has been developed in 1968 by Isacks and Oliver, called "New Global Tectonics". In the coverage of this theory, basic principles of mobile plates lithosphere, asthenosphere, subduction, volcanic arc systems etc) have been explained accomplishedly. In this theory, the production of lithosphere being started in mid-ocean ridges, while the destruction of the lithosphere being occurred in subduction zones. The controlling forces on this recycling mechanism of the Earth's plates has been shown in Figure 1.2.

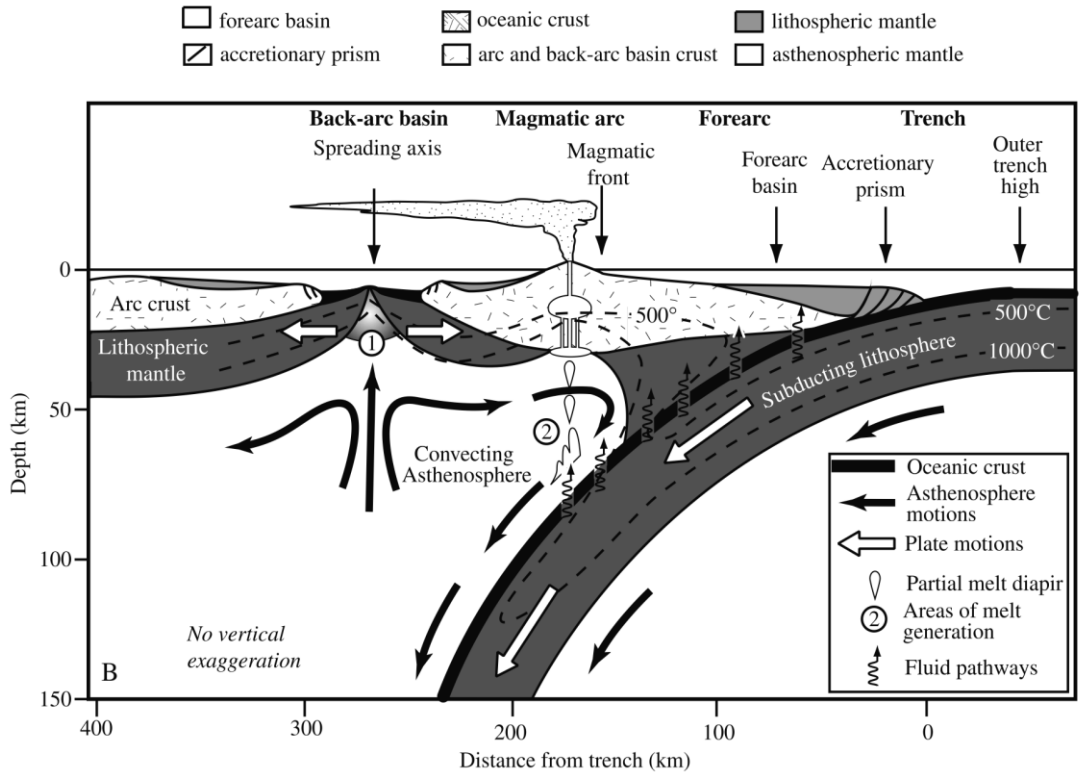

Figure 1.2 : The detailed illustration of the a subduction event and its governing forces. The minerals inside the being subducted slab generates melts and causes the formation of volcanic arc system over the hinge location. This processes followed by the back-arck extension. The carton obtained from Stern (2002).

1.3 Age of Lithosphere

J. Tuzo Wilson who Canadian geologist was discovered that the tectonic plate's recycling, also he stated the transform boundaries. This tectonic plate recycling process known as Wilson cycle. In this series of process an oceanic basin evolves by the means of the rifting and also it creates new oceanic plate by seafloor spreading. These plates are mobile due to push force which is imposed by ridge. When the plates move towards beneath the another plate, start to sink into plastic-like and less dense asthenosphere -if its sufficiently dense- and totally become disappear if the plate collide to another one. Owing to Wilson cycle we cannot find oceanic lithosphere older than ~180 m.y. (Pluijm and Marshak, 2004). However, the continental lithosphere is much older than oceanic lithosphere and also give us ideas the age of our planet. S. Wyche et al. (2004) found the oldest xenocrystic zircon than has previously been identified, in western Australia near the Yilgarn Craton. The results of zircon analysis

indicated that the oldest zircon crystal age range between 4.35Ga to 3.13 Ga. Figure 1.3 is show the significant events in Earth's lithosphere evolution.

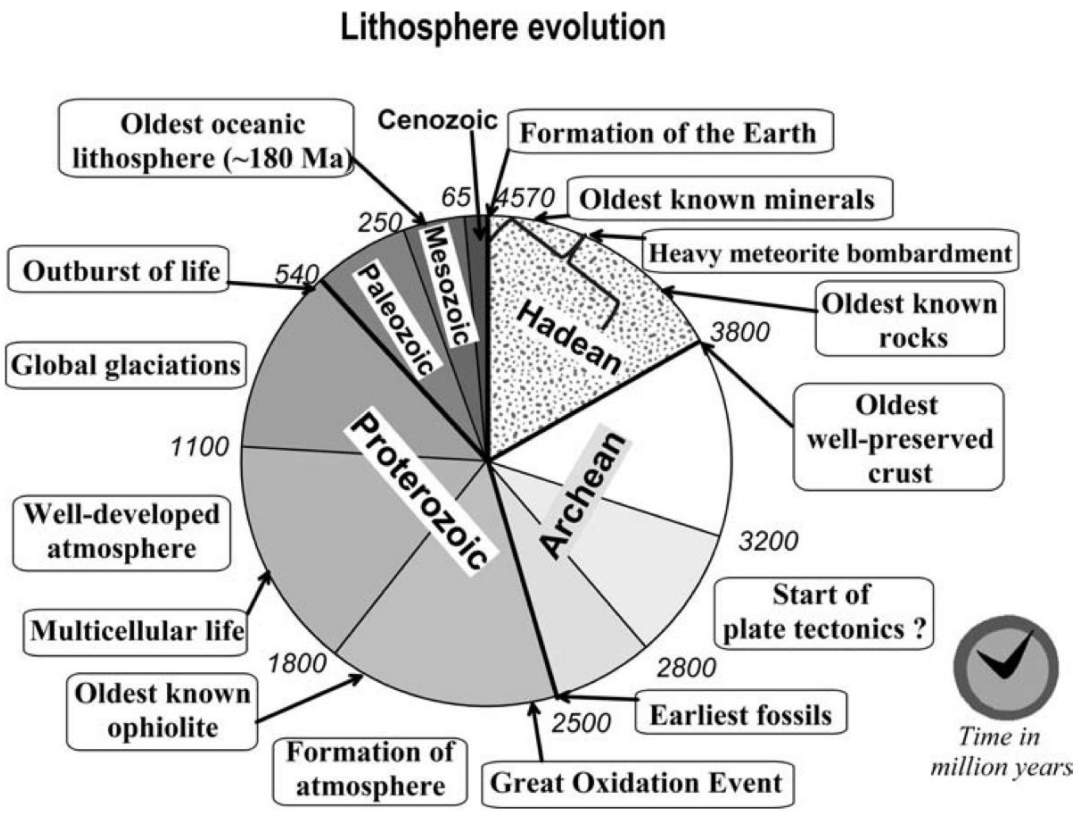

Figure 1.3 : The sketch shows the evolution of lithosphere within the geological time. Obtained from (Artemieva, 2011).

1.4 Plate Tectonics and Related Deformations

The Earth's lithospheric plates are not forever. They are destructed within time depending on thermal, physical and mechanical conditions and are recreated. This is because we can only observe to has survived plates until today by using geophysical surveys (Artemieva, 2011). The tectonic plates interact with each other in three different ways hence there are three types of tectonic boundaries: (1) convergent boundary; (2) divergent boundary; and (3) transform boundary. In convergent boundary zones (Eurasia-Arabia, India-Asia etc), two plates move towards each other. In divergent plate boundaries, two plates move away from each other and in transform plate boundaries, two plates slide pass one another. The lithospheric plates float on asthenosphere. The heat is transferred convectively inside plastic-like asthenosphere. Therefore, the asthenosphere both plastically flows and drags the lithospheric plates and causes the formation of processes which are give rise to large-scale lithospheric

deformations such as subduction, collision, delamination. The lithosphere is destroyed not only as mechanical and also can deform by thermally. There are four large-scale deformation types of lithosphere: (1) subduction; (2) delamination; (3) plume erosion; (4) Rayleigh-Taylor instability (Figure 1.4).

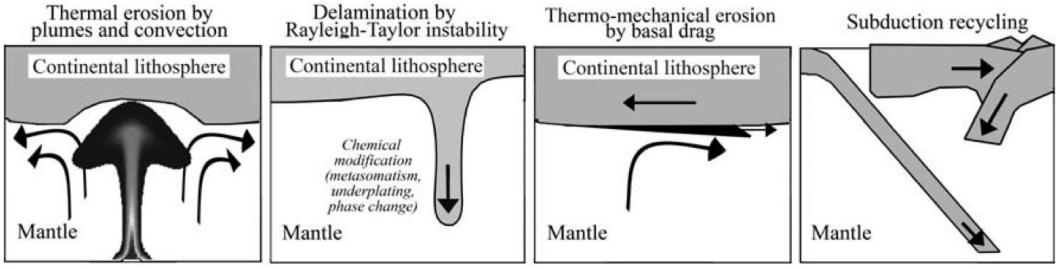

Figure 1.4 : The large-scale deformation types of lithosphere (Artemieva, 2011).

1.4.1 Subduction

The lithospheric plate which created in mid-ocean ridge is eventually thicken and also by cooling its become more dense than asthenosphere within the time. When it become sufficiently denser its begin to descent into asthenosphere. Closs (1993) found the plausible density contrast between lithosphere and asthenosphere to subduct as 10 cm/gr3. In the cases of the density contrast exceeds 10 cm/gr3 the lithosphere tends to subduct into the lighter and hot asthenosphere. There are several parameters that effects on subduction process such as age of being subducted slab, mantle abiadat, convergence rate, asthenosphere and overlying lithosphere composition and the mechanical properties of the lithosphere. Figure 1.5 shows the two different subduction evolution based on age of subducting slab.

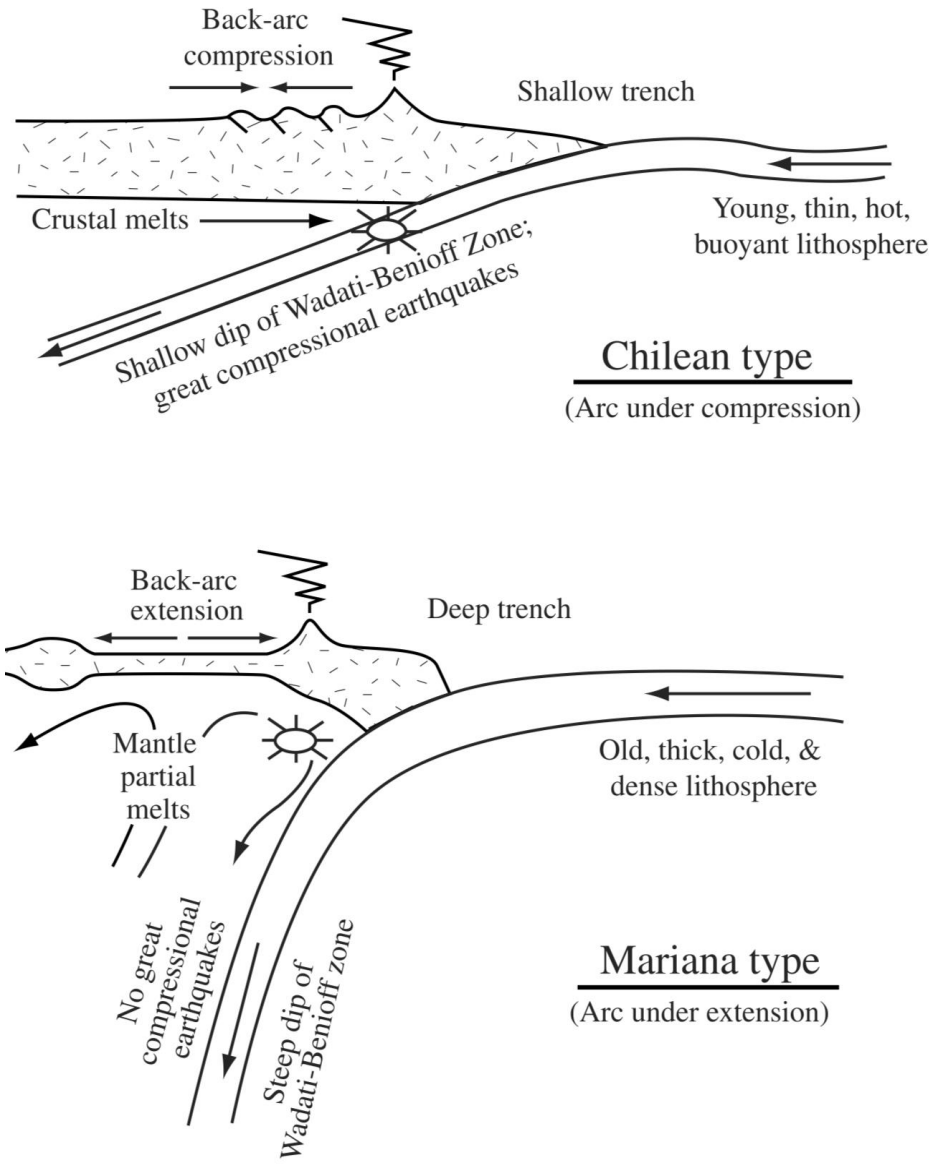

Figure 1.5 : The evolution of subduction as a function of age of the lithosphere. The sketch obtained from Stern (2002).

1.4.2 Delamination

The hypothesis of delamination refers to decoupling/peeling off of non-convecting uppermost mantle away from overlying crust (Bird, 1979). This peeling off of lithospheric mantle evolves as a dominant function of age of lithosphere, the rate of convergence –if any-, upper crustal thickness, lower crustal rheology and thermal properties of the transitional boundries (Moho surface etc.) (Bird, 1979; Bird, 1991; Kay et al., 1993). the colder hence denser uppermost mantle decouples from crust with its own weight and simultaneously replaced by plastic-like hot asthenosphere. This principle of decoupling in lithosphere facilitates that decoupling of the underlying

lithospheric mantle and plays a key role at the determining of the occurrence rate of delamination. However, although it is still controversial that the nature of lower crust, delamination hypothesis posists that deformation in the lower crust takes place viscously analogous to in jelly sandwich model (Referans, 1990). The occurrence rate of delamination is being change dependent on the heating rate of lower crust due to heat input to the base of the crust (Moho surface) via rising of asthenosphere.

1.4.3 Plume erosion

The lithosphere can deform thermally and convectively by upwelling mantle or mantle plume. The upwelling hot mantle material (1350 oC) rises until to the base of the lithosphere. The base of the lithosphere is start to weakening due to heat transferring its own inside by conduction. This is because why the high heat flow values are observed where in existed possible mantle plumes (Afar etc).

1.4.4 Rayleigh-Taylor instability

The Rayleigh-Taylor instability arise from the density competition between lithosphere and asthenosphere. This processes is often observed in convergence zones. In the first stage of the Rayleigh-Taylor instability, the crust thickens under the forces of compressional. The second stage is that increased load of crust causes bending of lithosphere into asthenosphere and takes place a lithosphere bulk. The mantle convection flows surround of the bulk and continues to deform and suck until its totally detachment from the base of the lithosphere.

1.5 Rheology

The “rheology” of a material is a term and defines the material responds against to affected force or imposed stress. The responses can be either recoverable or unrecoverable. The recoverable deformation describes that when the stress removed, the material can turn into its own original size, so the strain returns zero. However, in unrecoverable deformation, the material cannot turn into its original size. This is a permanent deformation such as faulting, cracking. Namely, the material’s response vary based on the imposed stress and the material behaves in four different ways: (1) brittle; (2) elastic; (3) visco-elastic; and (4) viscous/creep. We know that how the material behaves under different stress conditions from laboratory studies empirically.

1.5.1 Deformation types of a material

It is useful to state at the outset that the definations of stress, strain, strain-rate, strength to better understanding of the rheology of the Earth. Stress is force per unit area, affecting on a material. The unit of stress expressed as kilograms, pounds, tons, and so it. But, the strain develops as a result of applied stress and corresponds to change in the shape or volume of a material body. In fact, this is used to define the deformation of the material. The total strain variation with respect to the time interpret as strain rate (time dependent). The strength of a material is explained as the maximum diffential stress that the material can withstand to applied stress upon it.

The deformation of a material can describe by relationship between stress and strain. Strain is begin to vary if a stress factor imposed on a material/rock. This means the dimensions of material will show changes comparing to original size due to experienced deformation. The material will act according to the amount of applied force. In geology, the lithostatic pressure and temperature being increased with respect to the depth. Therefore, material's respond against to stress gradually changes from shallow to greater depths of crust due to significant variations in pressure and temperature. The stress deforms the material as permanently if it exceeds the material strength. In shallow level of crust, the material can turn into original size when the applied force is removed. However, if the material cannot turn into its original dimensions, the deformation called permanent/plastic/brittle. In general, permanent deformations take place by fracturing or faulting at shallow depths of crust. For this reason, the upper crust is classified as brittle deformed part of the lithosphere. Figure 1.6 shows that how a material deforms permanently under the affecting a stress factor. When the stress is exceeds the material strength, the material begins to rupture. This rupturing stress point known as yield stress or yield point or elastic limit. In this case, the brittle material deforms plastically. The another deformation type of the material called as elastic deformation in the upper crust. An elastically deformed material has ability to return its original dimensions when the stress is removed unlike plastic deformation in which there is a linear relationship between stress and strain in elastic deformation. But, occasionally a material body creeps when the stress is permanent. This deformation type is called visco-elastic deformation. The macroscopic fractures cannot observe in visco-elastically behaving body. If the creeping material body has a yield stress, the visco-plastic deformation occurs. In viscously deformed rocks, the

strain-rate is proportional to imposed stress. There is no crack or faulting or a yield point in this type of deformation. The rock/material creeps as a permanent deformation.

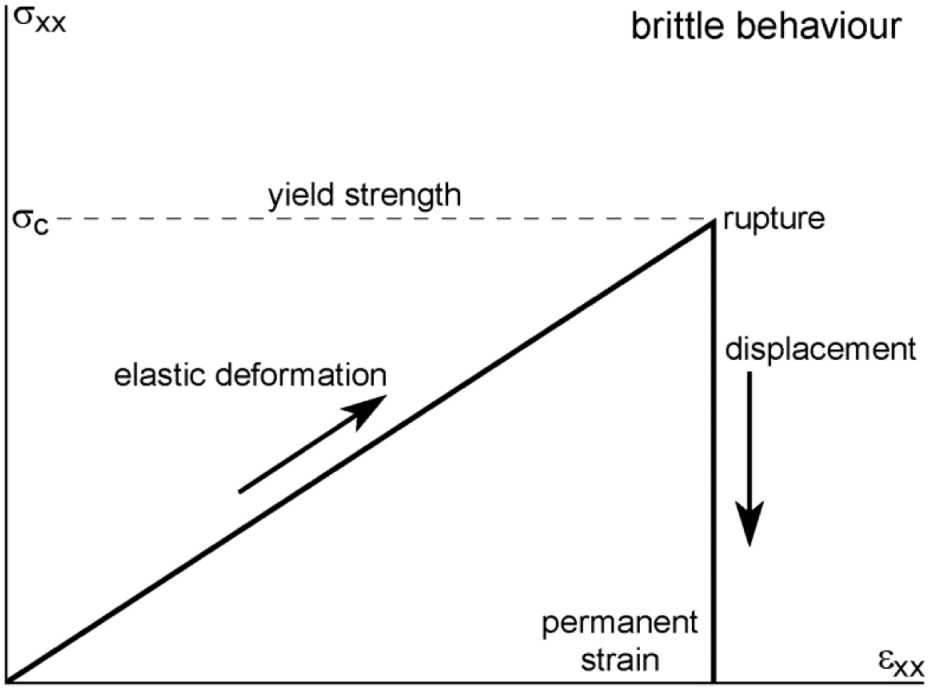

Figure 1.6 : The plot shows the relationship between stress-strain rate in a plastic material body. Yield stress corresponds to the material body ruptured in which stress point.

1.5.2 Thermal structure of lithosphere

The heat flow measurements per unit surface give the idea about the thermal structure of the lithosphere. The transferring of heat inside the lithosphere occurs via three ways: (1) hydrothermal circulation, (2) conduction and (3) convection. Figure 1.7 shows the how the heat transfers in which level of lithosphere (Artemieva, 2011). In Figure 1.7, it is clearly seen that the conductive transferring of heat dominate in crust. In the deeper level of lithosphere, the heat starts to transferring with convection, where is the lithosphere-asthenosphere boundary. Geophysical applications can measure only the conductive component of heat flow. The heat flow values are higher in oceanic lithosphere than in continental, because of the thickness of lithosphere. The heat loss energy during the transmission. The average heat flow data show that the mean global heat flow is approximately same or so close each other in oceanic and continental areas (Chapman, 2004). Only in some critical regions the heat flow is obviously higher such

as volcanic islands, mid ocean ridge, collision zones, where the large-scale lithospheric deformation occurred. In determination of heat flow, the crustal thickness and Moho temperature play a crucial role. The geotherm of the Earth can be divided into two different branch, cold and hot geotherm. The cold geotherm is observed the thick and old cratons and the Moho surface temperatures is around 550 oC. In the region where the hot geotherm is dominate, the Moho temperature can be exceed the temperatures of 800 oC. Table 1. shows the mean heat flux values in the crucial cites in the Earth.

Table 1.1 : The average heat flow measurements for different geological time series.

Archean	**$<Q>^a$(mWm^{-2})N_Q^C**	**$<A>^a$**	**Qab(nWm^{-3})N_A^C**	**References**
Dharwar (India)	36			Roy and Rao (2000)
Kaapvaal basement (S. Africa)	44	1,8	-	Ballard et al. (1987), Jones (1988)
Zimbabwe (S. Africa)	47	1,34	-	Jones (1987)
Yilgarn (Australia)	39	3,3	-	Cull (1991)
Superior (N. America)	41	0,72	0,73	Mareschal et al. (2000)
Wyoming (N. America)	48.3	2,3	1	Marechal et al. (2004)
Total Archean	41	3,1	2,1	Decker et al.(1980)
Proterozoic				
Aravalli (India)	68			Roy and Rao (200)
Namaqua (S. Africa)	61	2,3		Jones (1987)
Gawler (Australia)	94	3,6	-	Cull(1991)
Sao Fransico craton (Brazil)	42	1,5	0,6	Vitorello et al. (1980)
Braziliane mobile belt (Brazil)	55	1,7	1,2	Vitorello et al. (1980)
Ukrainian Shield	36	0,9	0,2	Kutas (1984)
Trans-Hudon (N. America)	42	0,73	0,5	Rolandone et al. (2002)
Wopmay (N. America)	90	4,8	1	Lewis et al.(2003)
Grenville (N.America)	41	0,8		Mareschal et al.(2000)
Total Proterozoic	48			Nyblade and Pollack (1993)
Paleozoic				
Appalachians (N.America)	57	2,6	1,9	Jaupart and Mareschal (1999)
Basement United Kingdom	49	1,3	0,5	Lee et al. (1987)
Urals	30			Kukkonen et al. (1997)
Total Paleozoic	58.3			Pollack et al. (1993)

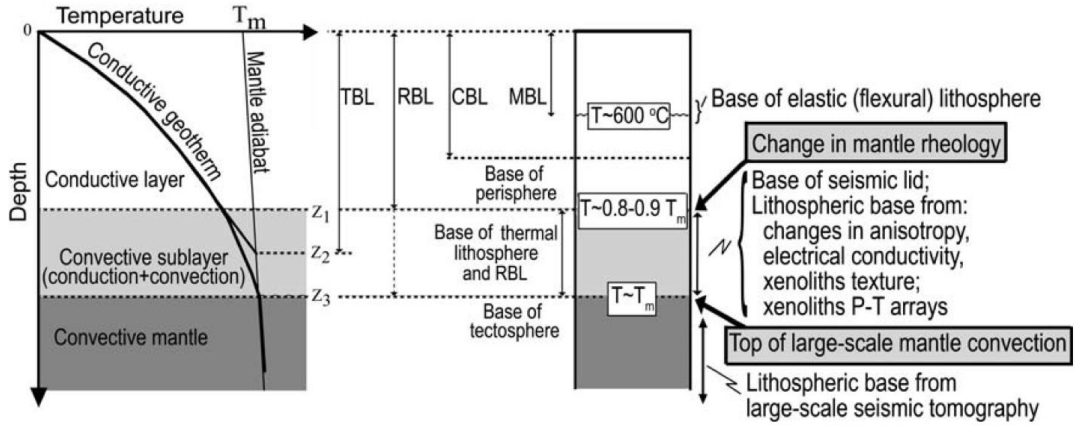

Figure 1.7 : The bases of layers at the lithosphere and the types of heat transfer in each layer [1].

1.5.3 Rheology of lithosphere

For different tectonic settings and lithospheric age, there are several types of lithosphere rheology considered as heterogeneous (layered) and homogenous (olivine); and the lithosphere deformation is occurred as elastic, elastic-plastic, viscoelastic (Kirby and Kronenberg, 1987). In lithosphere scale deformation rheology varies based on the composition of the rocks and the thermal state of the lithosphere. These parameters specify that how the lithosphere will be deform during a tectonic episode (semi-brittle, plastically, visco-plastic, creep etc). Temperature and lithostatic pressure are the main controller parameters how the rheology of lithosphere will develop. This is because we see different rheology at the same Earth. Also the thermal state/ geotherm is changes the rheology of the lithosphere. The dependency of viscosity to temperature is significant in terms of the deformation and this causes the consideration of more complex structure.

2. BRIEF INFORMATION ON NEOTECTONICS OF TURKEY

Turkey is one of the most active tectonic zones in the Earth. The neotectonics of Turkey is formed by three geodynamic events: (1) African subduction beneath the Aegean; (2) transform faults of North Anatolian Fault and East Anatolian Fault and those relation with tectonic escape of Anatolian micro-plate; (3) East Anatolian collision zone, as a result of Arabian plate's northward propagation to Eurasia – relatively stable to the Arabia-. The tectonic framework mapped out and shown in Figure 1.8. According to this map (Bozkurt, 2001), while the west side of Turkey is characterized by extensional deformation due to subduction, the east side of Turkey characterized by contractional deformation owing to collision of Arabian plate to the east Anatolia. The another subject is that the escape of the Anatolian micro-plate via transform faults NAF and EAF. The NAF is around at 1500 km-long, dextral strike-slip fault and extends until to Greece, the width of the fault zone ~40 km (Bozkurt, 2001). The geological data suggest that the NAF displacement is around 2 cm/yr and total displacement is 85 km (Bozkurt, 2001). The EAF is left lateral transform fault and similar to NAF also its promotes the westward escape of Anatolian micro-plate. There are three proposed model for evolution of tectonic escape in Turkey: (1) gravitational collapse; (2) northward subduction of African plate beneath Aegean region and its caused slab pull force; (3) collision of Arabian plate to Eursia along Bitlis-Zagros suture zone.

The structural geology of Turkey is evolved in the agreement with the current geodynamic setting. The west side of Turkey is extensional provinces so that the normal faults and related structures are dominated to the region such as Menderes Massif. However, there is a different geodynamic history in the east side of Turkey depending on the collision and pre-collisional oceanic province of Neo-tetys. There was an ocean between Arabian and Eurasia before collision (~13 Ma), named Neo-tethys. This ocean has been terminally closured by the collision of the Arabian plate, and the contractional regime has been started. As a result of this regime, the east Anatolian Plateau has uplifted around 2 km above the sea level. With this elevation,

the East Anatolia exhibits a high plateau characteristics as a part of Alp-Himalaya mountain belt.

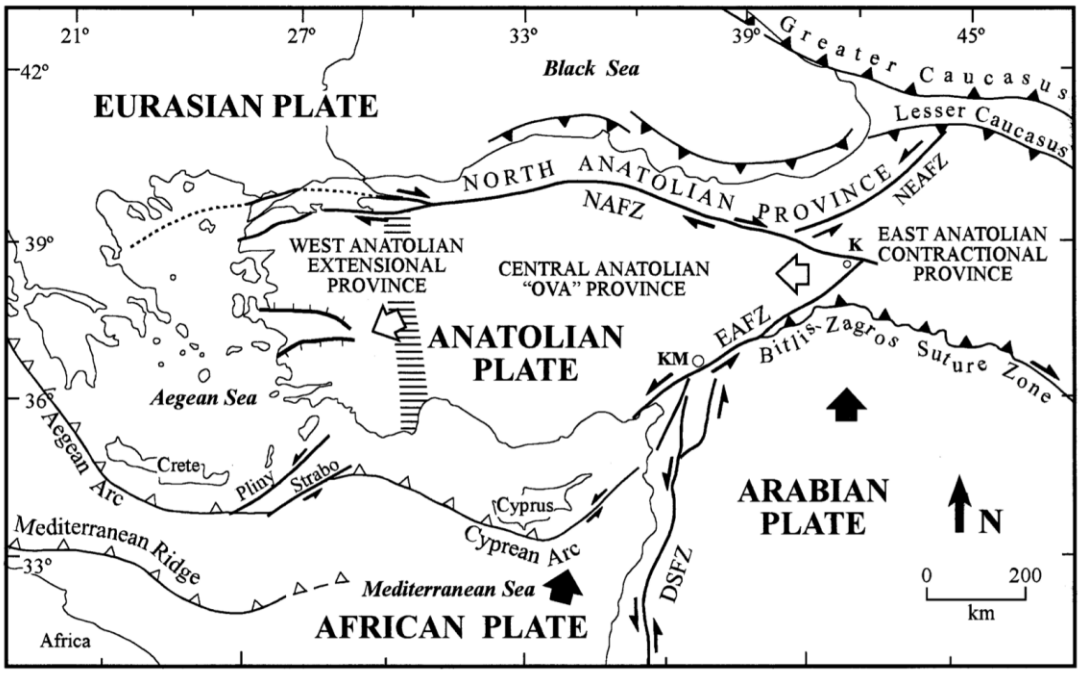

Figure 2.1 : Tectonic framework of the Anatolia, the map obtained from Bozkurt (2001).

3. EAST ANATOLIAN HIGH PLATEAU

Geophysical studies reveal that most of the orogenic regions are devoid from non-convective part of mantle, where most likely delamination occurred (Apennines, southern Tibet, the Carpathians, Alpino, Colorado etc.). In such regions, delamination is hypothesized to account for rapid uplift, mafic magmatism, extension and reduced seismic wave (Bird, 1979). The east Anatolian High plateau exhibits these expected consequences of delamination. The region is being rised since middle Miocene and today stands at around 2 km elevation above the sea level. Moreover, high heat flow values (Aydın et al., 2005; Pamukcu et al., 2014), reduced seismic waves (Zor et al., 2003; Angus et al., 2005; Ozacar et al., 2008; Özacar et al., 2010) and negative bouger anomaly (Barazangi et al., 2006; Seber et al., 2005; Schildgen et al., 2014) are imply that unstable and deformed lithospheric conditions beneath the east Anatolia.

These geophysical and geological observations make the EAHP a crucial cite that likely experienced delamination and following slab- break off (Şengör et al., 2003).

In this study, by performing 2d geodynamic experimental code SOPALE (Fullsack, 1995), we conducted a series of geodynamic experiments consist of four stages. In the first stage of the experimental series, we determined that which lower crustal rheology (diabase, felsic granulite, mafic granulite etc.) is more plausible for delamination of mantle lithosphere. In the second stage of the experimental series, we used different plate convergence rates (1 to 5 cm/yr) and mantle lithosphere plasticity values (30 to 120 MPa) to observe variations on long-term slab dynamics (slab break-off etc) as much as its effects on crust and topography. In the last stage of experimental series, we detect the mantle lithosphere failure stress values (MPa) that allow to slab break-off . We also considered that the dynamic effect of the slab break-off on the surface topography. Eventually, all model results are evaluated inclusively and compared with the observations of Eastern Anatolia to figure out influences of delamination processes and its ability at plateau growth.

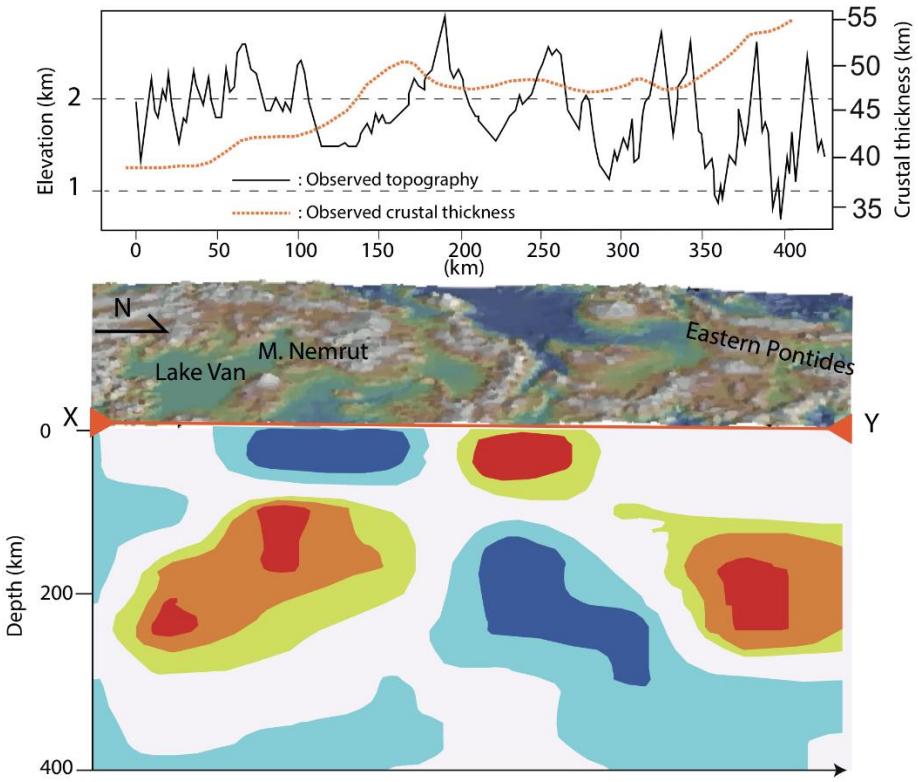

Figure 3.1 : Seismic tomography image beneath the east Anatolia. The tomographical cross-section modified from Lei and Zhao, 2007. The plot above the image shows the observed crustal thickness (Zor et al., 2003) and the topographic profile (Geomapp v1.2).

Deep seismic images reveal that the mantle lithosphere is completely absent or so thin below the east Anatolia (Primollo and Morelli, 2003; Lei and Zhao, 2007; Gök, 2007; Zor, 2008; Bozdağ et al., 2012). Figure 1.9 shows that the mantle lithosphere-like material (blue) is not attached to the base of the crust below the EAHP and no connection with Arabian lithosphere.

On the other hand, petrological findings also emphasize that presence of irregularities at sub-lithospheric conditions. Whole region is characterized by wide-spread volcanism since middle Miocene. Isotopic dating results show that the volcanism has begun in Erzurum-Kars plateau (north, EKP) up to 13 Ma, afterward volcanism started to southward migration switching in chemistry from calc-alkaline to alkaline (Keskin, 2003). Volcanic rocks are mostly cal-alkaline and midly alkaline, where in Erzurum-Kars plateau and Eastern Pontides, whereas volcanic products of Muş-Nemrut-Tendürek volcanoes are mostly in alkaline chemistry to the south, apperantly the alkalinity increasing to the south (Keskin, 2007). Additionally, it is reported that there

are transitional volcanic centers such as Bingöl and Süphan volcanoes (Pearce et al., 1990).

These geophysical and geological observations make the EAHP a crucial cite that likely experienced delamination and following slab- break off (Şengör et al., 2003).

In this study, by performing 2d geodynamic experimental code SOPALE (Fullsack, 1995), we conducted a series of geodynamic experiments consist of four stages. In the first stage of the experimental series, we determined that which lower crustal rheology (diabase, felsic granulite, mafic granulite etc.) is more plausible for delamination of mantle lithosphere. In the second stage of the experimental series, we used different plate convergence rates (1 to 5 cm/yr) and mantle lithosphere plasticity values (30 to 120 MPa) to observe variations on long-term slab dynamics (slab break-off etc) as much as its effects on crust and topography. In the last stage of experimental series, we detect the mantle lithosphere failure stress values (MPa) that allow to slab break-off . We also considered that the dynamic effect of the slab break-off on the surface topography. Eventually, all model results are evaluated inclusively and compared with the observations of Eastern Anatolia to figure out influences of delamination processes and its ability at plateau growth.

3.1 Information on Geology and Geodynamics of East Anatolia

The east Anatolia collision zone has identified as a part of Alp-Himalayan orgenesis belt and comprises of three main units, which are separated by suture zones. Figure 3.1 shows the geologic units and related tectonic boundaries along the east Anatolian plateau.

The history of the geodynamic evolution of the east Anatolia region begin with the northward elemination of the northern branch of Neo-Tetys oceanic lithospheric mantle beneath the eastern Pontides. As the results of this subduction; (1) an accreated terrane (the east Anatolian Accreanary Complex, EAAC) took place by the peeling off the crust and its accumulation above that being subducted Neo-Tethyan slab and (2) it has been triggered the arc-type volcanism between Late Jurassic to Cretaceous hence the volcanic rocks in calc-alkaline composition dominated in the eastern Pontides (Pearce, 1990; Yılmaz et al., 2010). Izmir-Ankara-Erzincan suture zone (IAESZ) set aparts the eastern Pontides from the Eastern Anatolia Accreationary Complex

(EAAC). This is a large subduction-accreation complex and covers the area, where between the Eastern Pontides and the Bitlis massif. This unit contains the ophiolites and ophiolitic melanges pre-Jurassic to pre-Albian in age near the IAESZ to the north (Yılmaz et al., 2013). The ages of ophiolites and ophiolitic mélanges show younging from north to the south (Topuz, 2014). One of the most important rock community is that shallow marinal Adilcevaz limestones, resides in around 1.5 km elevation above the sea level within the EAAC. The dating results of the fossils in Adilcevaz limestones indicate that the closuring of northern branch of Neo-tethys ocean has been completed in Serravalian (11 to 13Ma), namely there was no sea water in the eastern side of Anatolia after mid-Miocene (Demirtaşlı and Pisoni, 1965; Gelati, 1975; Yılmaz et al., 1997; Şaroğlu ve Yılmaz, 1987; Şengör et al., 2008). This means the eastern Anatolia High Plateau might be begun to uplift synchronously with terminal closure of Neo-tetys' northern branch and following Arabian collision (Şengör et al., 2003; Şengör et al., 2008). Bitlis Massif being formed the southern part of the region and exhibits a pre-detached terrain properties from the Arabian foreland during the closure of the southern branch of Neo-Tethys Ocean. This terrain has stacked and been methamorpzed afterwards the Arabia-Eurasia collision. However, based on observed variety at P/T phases (HP/LT-LP/HT), Oberhânsli (2010) considered that the Bitlis massif was exposed to a series of subduction events, likely at least two times.

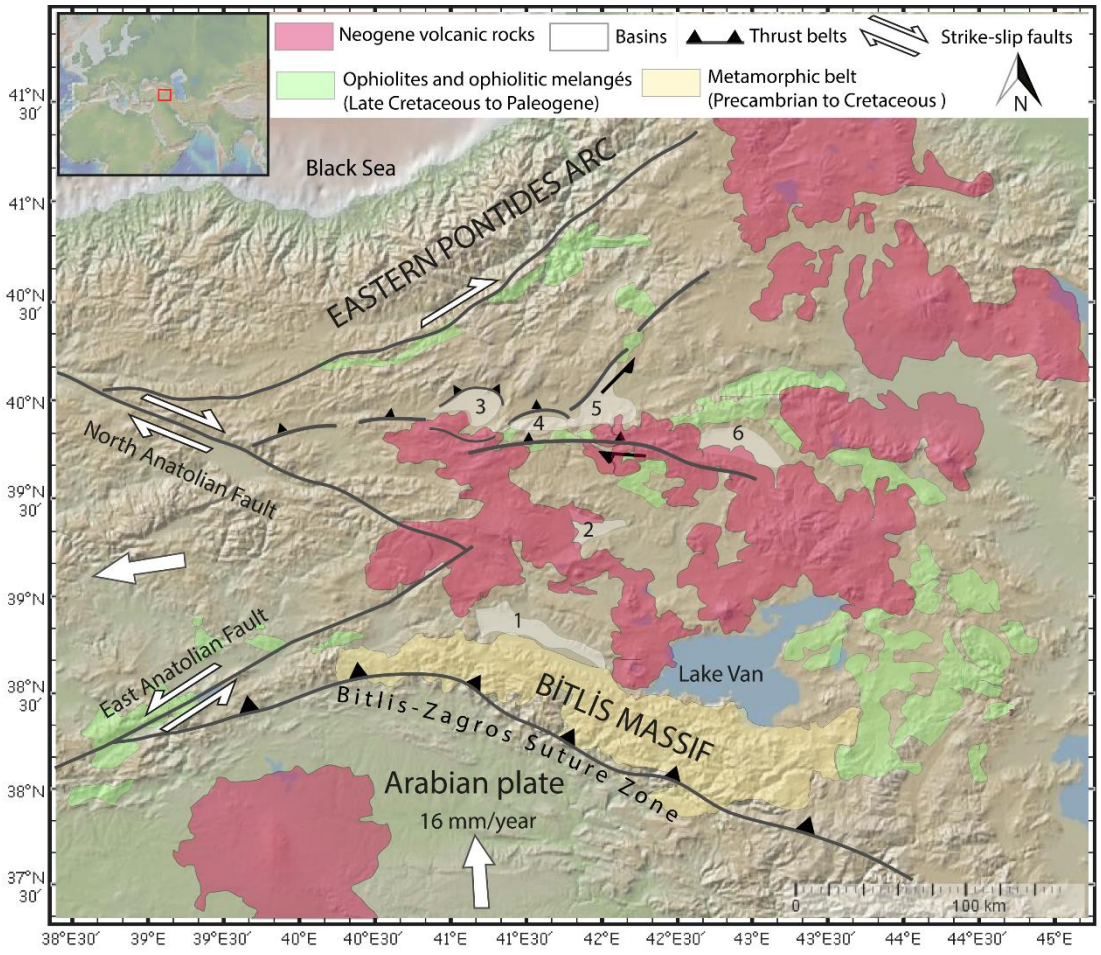

Figure 3.2 : Geological map of the east Anatolian High Plateau. The map modified from the GCME's (Geological Commission of the Middle East) map and Şengör et al., 2003.

3.2 Modeling Delamination

3.2.1 Former modeling studies

The hypothesis of delamination refers to decoupling/peeling off of non-convecting uppermost mantle away from overlying crust (Bird, 1979) as a result of its negative buoyancy. The decoupled mantle lithosphere simultaneously replaces by hot asthenosphere and this results in rapid uplift of topography, mafic volcanism, reduced seismic waves and negative gravity anomaly. Even so there are a great number of publications, in which state the controlling rheological, mechanical and thermal factors of large-scale deformation mechanisms of lithosphere, our main knowledge subjected to delamination hypothesis is still very conceptual to infer that how delamination initiates.

The geodynamic modeling studies are make it quite effective that to understand the complexities at lithospheric scale deformation and its consequents. In the past decade, we could provide a better understanding of delamination process by means of the progress on geodynamic modeling studies. A vast number of articles subjected to geodynamic modeling of delamination have been published to explain its setting parameters (rheological, physical, compositional etc.) and post-delamination anomalies (high heat flow, reduced seismic waves etc.) from deep mantle to the surface (Duretz and Gerya, 2013; Gerya et al., 2001; Göğüş et al., 2008; Göğüş et al., 2011; Magni et al., 2013; Morency and Doin, 2004; Ueda et al., 2012). In these sequences of publications, a number of rheological, mechanical and physical parameters have been tested and they obtained quite identical results. Göğüş et al. (2008) argue that whether delamination may responsible for development of extensional basins in convergence zones. Likewise, Duretz and Gerya (2013) show that the retreat of decoupled lithospheric mantle promotes development of such extensional areas until its break-off. On the other hand, Magni et al. (2013) investigate that the influence of changes in viscosity of lower crust and lithospheric mantle. They found that mechanical decoupling/coupling and detachment of lithospheric mantle occur mainly based on viscosities of lower crust and lithospheric mantle. More specifically, by using different temperatures at the base of the crust, Morency and Doin (2004) specify that an inverse relationship between activation energy of lower curst and rapidity of delamination.

3.2.2 Method and model setup

In this study, we used SOPALE a plane strain visco-plastic finite element code (Fullsack, 1995; Pysczklewec, 2012) that computes and visualize the flow of visco-plastic materials. The governing formula is that to measure the responds to creep:

$$\eta e\,(\dot{\epsilon}\,, T) = A^{-1/n}\,\dot{\epsilon}^{1-n/n}\,e^{Q/nRT} \qquad (1)$$

Here in the formula, ; strain rate, T; temperature, σ; diferantial stress, A, n, Q and R are viscosity parameters, power law exponent, activation energy and ideal gas constant.

Our models conducted to explore: (1) the coupling between various lower crustal rheology and lateral delamination speed; (2) plastic yield limits of mantle lithosphere to break-off; (3) impacts of plate convergence rate; (4) the ability of delamination at

plateau growth including possible mechanical effects of upper crust and mantle lithosphere, at different compositions of lithosphere and crust.

The initial configuration of model is (Figure 3.2) produced to simulate delamination as one-sided. The horizontal and vertical dimensions of the box is 2000 km and 660 km, respectively. The visualization of creeping flow is reorganized by the moving of the Eularian grids (201x101). The Eularian grids contain the needed information for the calculation of velocity, temperature field and pressure, while the Lagrangian grids (601x301) are moved along a pattern by recording physical history of material particles (temperature, pressure etc).

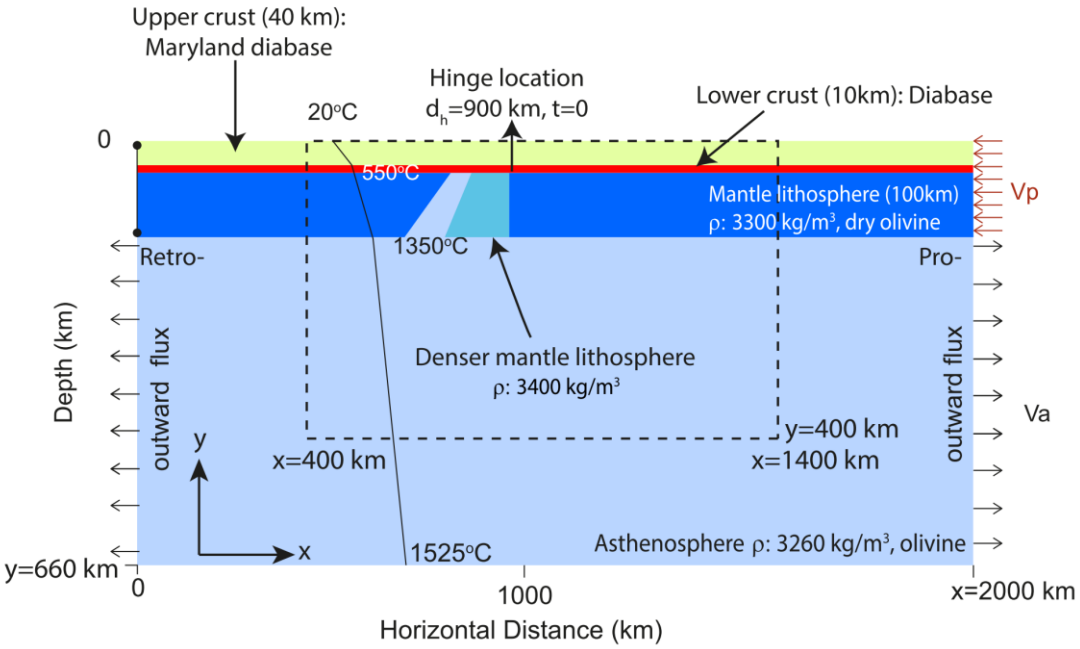

Figure 3.3 : The model initiation setup. The physical properties of the layers and the references of the used creep parameters belonging to materials has been shared at Table 3.1. In continental basement models, the rheology of upper crust is quarzite (from Gleason and Tullis,1995), while in oceanic basement models the rheology of upper crust has been choosen as diabase (from Ranalli, 1995), however, its effective vicousity has been scaled down by a factor of 0.2 to resemble an oceanic crust. Pro- and retro-side mantle lithosphere represent, Arabian plate and Eurasian plate, respectively.

In the models, the initial geotherm is held fixed by a surface temperature 20 oC, 550 oC at Moho, 1350 oC at lithosphere-asthenosphere boundry (LAB) and 1525 oC at bottom of the box.

An oceanic part (100x100) has been attached on the toe of the delaminating mantle lithosphere to represent Neo-tetys oceanic lithosphere. On the other hand, the oceanic

part also favors to separation of mantle lithosphere away from crust, by creating slab pull force and its no dynamic effect on evolution after 5 Myr from model initiation. The upper crustal and mantle lithosphere thickness show a change systematically, however, the lower crustal thickness is fixed at 10 km. Physical creep parameters and densities pertaining to materials given at Table 2.

In the models, the convergence rate ranging between 0 to 5 cm/yr and imposed from right side of the box. The topside of the box treats as a dynamic surface, while the bottom-side of the box is fixed. The mass balance of the models provided by outward flux of asthenosphere which is being change depending on both the convergence rates and lithosphere thickness. The rate of the outward flux is change between 3.17 cm/yr-15.85 cm/yr.

Table 3.1 : The physical parameters of the models

Mechanical Parameters	Upper Crust	Lower Crust (weak zone)	Mantle Lithosphere	Asthenosphere
Density,(kg/m^3)	2840	2990	3300	3260
Ø1(deg.)	15	15	0	0
Ø2(deg.)	2	7	0	0
$(I'_2)^{1/2}$	0,5	0,5	0,5	0,5
$(I'_2)^{1/2}$	1	1,25	1,5	1,5
Cohesion (Mpa)	100	0	90	100
Rheology	Quartz	Felsic granulite	Olivine	Olivine
Reference	Gleason and Tullis (1995)	Mackwell et al. (1998)	Hirth and Kohlstedt (1996)	Hirth and Kohlstedt (1996)
A($Pa^{-n}s^{-1}$)	$1.1x10^{-28}$	$8x10^{-21}$	$4.89x10^{-17}$	$4.89x10^{-17}$
n	4	4	3,5	3,5
Q,(kJ/mol)	223	485	515	515
Heat capacity,(J/kgK)	793	793	793	793
Thermal conductivity,(W/mK)	2,25	2,25	2,25	2,25
Thermal expansion,(K^{-1})	$2x10^{-5}$	$3x10^{-5}$	$2x10^{-5}$	$2x10^{-5}$
Radioactive heat production,($\mu W/m^3$)	0	0	0	0

3.2.3 Rheology of Lower Crust vs Lateral Delamination Speed

It is widely accepted that this peeling off the lithospheric mantle evolves as a dominant function of rate of convergence –if any-, upper crustal and lithospheric mantle thickness and those thermal and rheological properties (Bird, 1979; Bird, 1991; Kay et al., 1993). In addition, delamination hypothesis posists that the existence of a weak (ductile) mid-to-lower crust between two strong layers (upper crust and lithospheric mantle) analogous to "Jelly Sandwich Model". Parallel to this, Jull and Kelemen (2001) by using different lower crustal and mantle bulk compositions show that lower crustal density decreases and becomes weaker at higher Moho temperatures exceeding

of 800 oC. Such high temperatures at Moho surface are observed in response to: (1) thickened crust along post-collisional zones and (2) heat inputing to the base of the crust due to upward hot sub-lithospheric material migration as a consequent of peeling off the lithospheric mantle. This rheologically weaker and deep crustal layer plays a key role at the regulation of lateral delamination speed. As the delaminated mantle lithosphere warm, the separation of lithospheric mantle will be more rapidly and easier due to weakening at rheology of lower crust (Bird, 1991; Burov, 2011; Magni et al., 2013). Another factor that would be influence to the lateral delamination speed that is introducing of continental crust into asthenosphere together with lithospheric mantle. In this case, the buried crustal material into asthenosphere will resists to sink as a result of its positive buoyancy, so that the lateral delamination speed will decrease (Duretz and Gerya, 2013; Meissner and Money, 1998; Regard et al., 2008).

In the first stage of this study, we test that how does the lower crustal rheology affect the lateral delamination speed. Different sets of viscous flow law parameters (Ranalli, 1995) belonging to lower crust are used (diabase, mafic granulite, felsic granulite, diorite) (Table 3.2). For each rheology of lower crust, we calculated an avarege delamination speed (km/Myr) by measuring the lateral distance between the initial (t=0) and terminal (t=18 Myr) delamination hinge locations (Figure 3.2). Note that lithosphere thickness held fixed by 140 km (30 km: upper crust, 10 km: lower crust, 100 km: mantle lithosphere) and not imposed plate convergence from pro-plate side.

We used the term of delamination hinge to define that location of the thickest point in the upper crust. This localized point in upper crust corresponds to vertical projection of the location at surface (z=0 km), where the pro-plate mantle lithosphere is bended. The crust thickens under the control a tensional force, which is imposed by the delaminated mantle lithosphere in direction of gravitational acceleration. Moreover, delamination hinge point moves together with ongoing delamination of pro-plate mantle lithosphere either by advancing or retreating as reported by Gerya et al., (2013).

Table 3.2 : Physical parameters for different lower crustal rheologies, taken from Ranalli, 1995.

Material	A(MPa-ns-1)	n	E(kJ mol-1)
Diabase	2.0x10-4	3,4	260
Felsic granulite	8.0x10-3	3,1	243
Mafic granulite	1.4x104	4,2	445
Peridotite (wet)	2.0x103	4	471

In the models, it is clearly seen that the amounts of delamination hinge displacement show discrepancy by switching of lower crustal rheology (Figure 3.2). The highest hinge displacement occurred when the rheology of lower crust selected as felsic granulite (Figure 3.3). In this case, delamination hinge has retreated ~230 km within 18 Myr (Figure 3.3). When the rheology of the lower crust chosen as diabase or mafic granulite the amount of hinge displacement decreases to 118 km and 50 km, respectively (Figure 3.3). On the other hand, we realized that the separation of pro-side mantle lithosphere tends to be easier in the case of decreasing at activation energy of lower crustal rheology, as mentioned in Magni et al (2012). Owing to selection more strong lower crustal rheology, the amount of migration has decreased. The resist has been increased to decouple of pro-plate mantle lithosphere so that occurrence speed of delamination will decrease. Therefore, we decided to use felsic granulite rheology in lower crust.

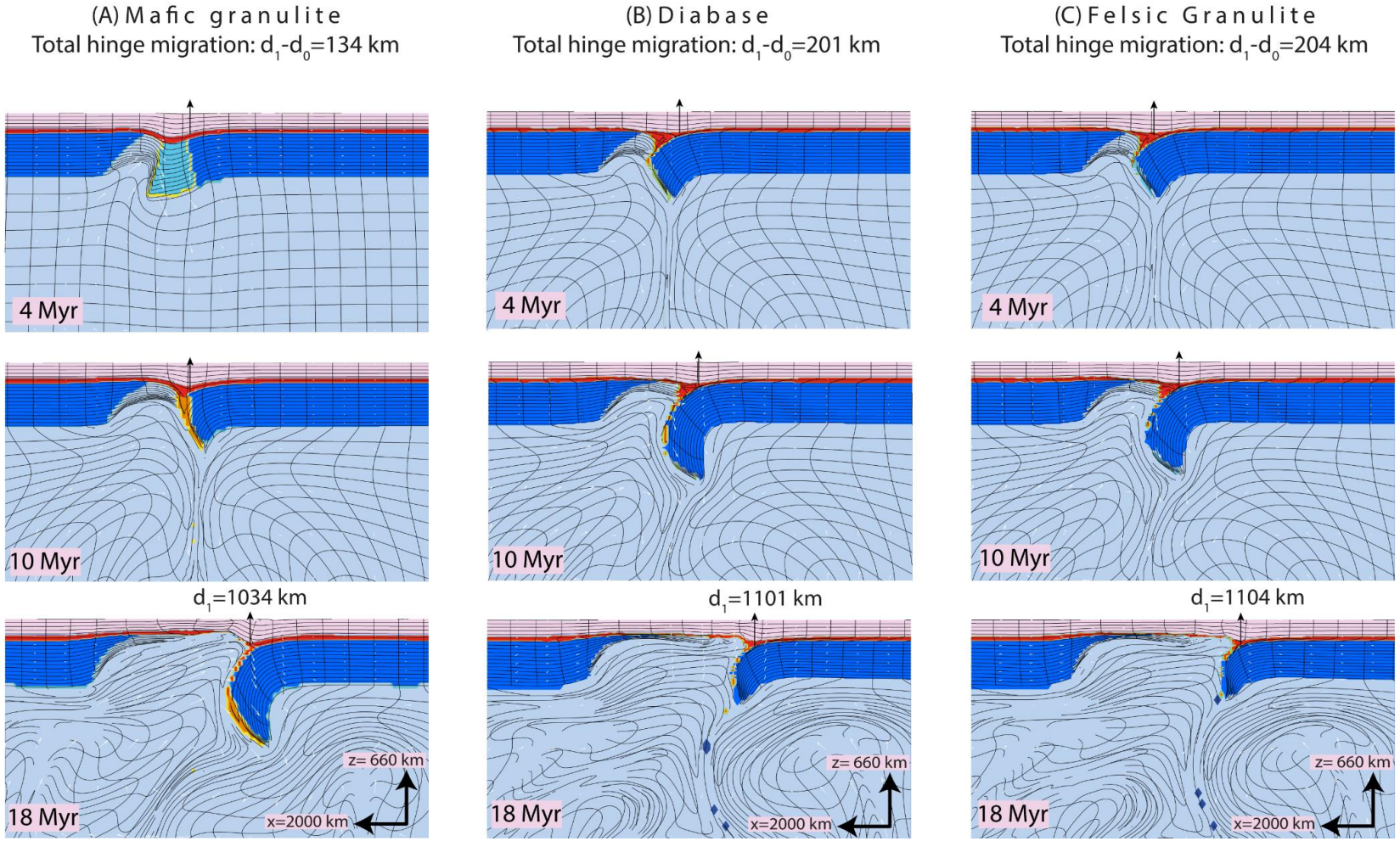

Figure 3.4 : The geodynamic evolutions of delamination event in the case of the using different lower crustal rheologies: (a) diabase; (b) mafic granulite; (c) felsic granulite. The delamination hinge migration amounts has been plotted at Figure 4.2.

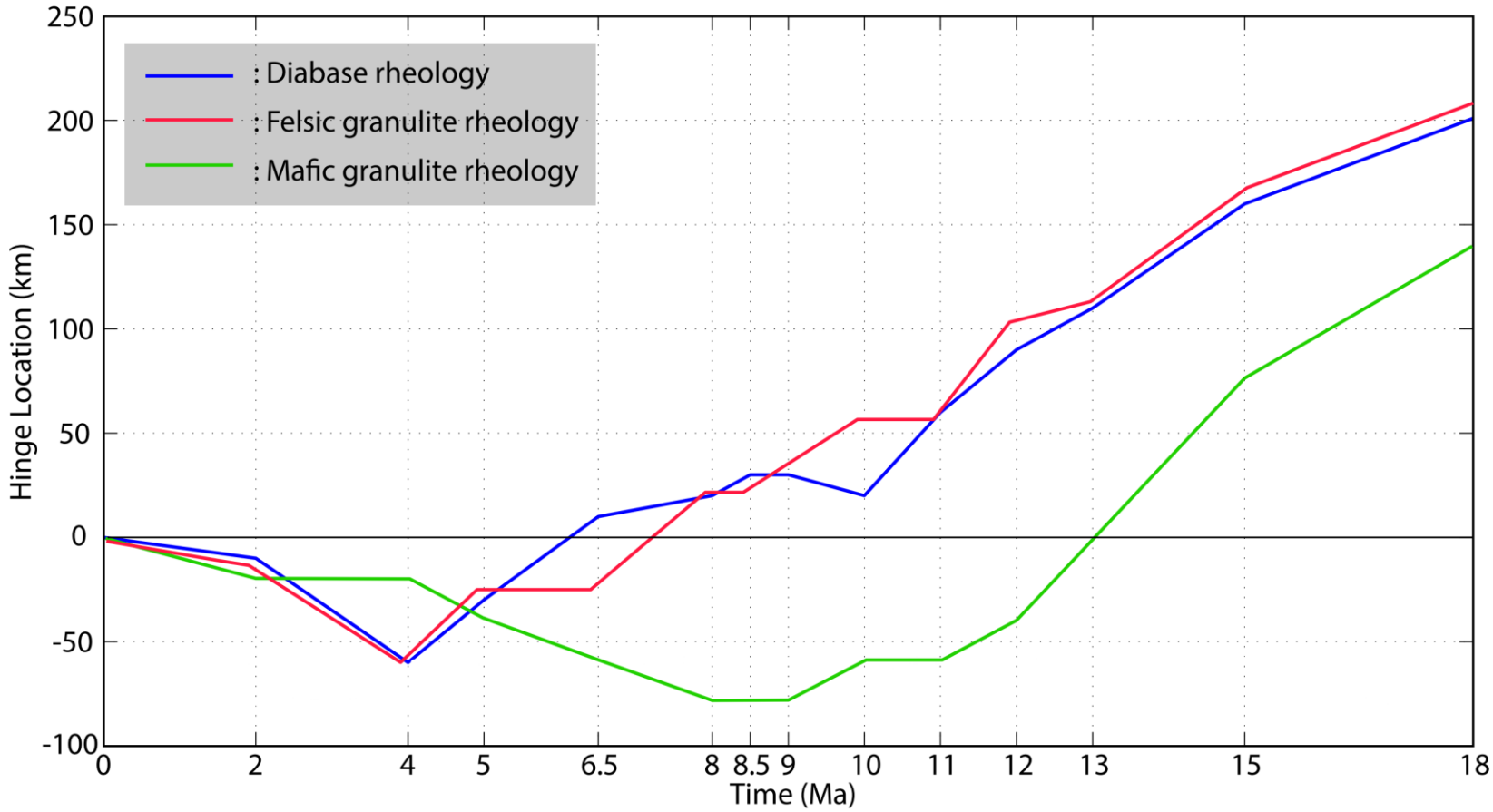

Figure 3.5 : The plot in (a) shows the geodynamic evolution of delamination in 18 Myr when the lower crustal rheology selected as diabase; (b) shows the geodynamic evolution of delamination in 18 Myr when the lower crustal rheology selected as mafic granulite; (c)

.

4. EXPERIMENTAL RESULTS

4.1 The Evolution of Lithospheric Delamination in Continental Basement

Reference Model

In the reference model (Figure 4.1), we only imposed a convergence rate of 2 cm/yr from the right side of the box and plastic yield stress of 90 MPa is used for the mantle lithosphere at either side. The continental mantle lithosphere consists of 40 km in thick upper crust, 10 km in thick lower crust and 100 km in thick mantle lithosphere. The rheologies are determined as wet quartz in upper crust (Gleason and Tullis, 1996), felsic granulite in lower crust (Mackwell et al., 1998) and olivine in mantle lithosphere (Hirth and Kohlstedt, 1996). Reference densities of upper crust, lower crust and mantle lithosphere is 2840 kg/m3, 2990 kg/m3 and 3300 kg/m3, respectively. At the t= 4 m.y., the oceanic (Neo-tetyhs) mantle lithosphere part has started to sink downward and lied to pulled down its attached mantle lithosphere, which is corresponds to Bitlis-Pötürge slab (Figure 4.1). The downward motion give rise to screcthing the crust vertically over the delamination hinge, denoted with 'dh'. At this moment, crustal thickness has increased about 50 km at the hinge location. At t= 5 m.y., the representing to Neotetys oceanic part has detacthed from toe of the Bitlis-Pötürge slab and replaced by asthenospheric material. The surface topography is uplifted/rebounded (from -2 to +2 km) as localized over the hinge point by rising of the hot asthenosphere and removal of load. Following this topographic undulation, at t= 6.5 m.y., the delamination has begun. From this moment, the crustal thinning also has started owing to stretching of crust as consequent of rising hot asthenosphere instead of decoupled mantle lithosphere. Convective flows denoted with white coloured arrows inside the box (Figure 4.1) and clearly indicate that the intrusion of asthenosphere into weak lower crust. This provides the peeling of the pro-side mantle lithosphere and tends to enhace within the model duration.

At time t= 12 m.y., the decoupled mantle lithosphere has bended and steepened into asthenosphere. At this moment, the maximum surface topography is up to 2 km, however; there is a negative surface topography ~ -2 km beneath the hinge location

owing to tensional force, which is imposed by the decoupled mantle lithosphere. At t=15 m.y., the decoupled mantle lithosphere is detached and second topographic undulation is observed. The tensional force diminished by break off the pro-side mantle lithosphere so that topography rebounds upward, it causes creating of a positive topography.

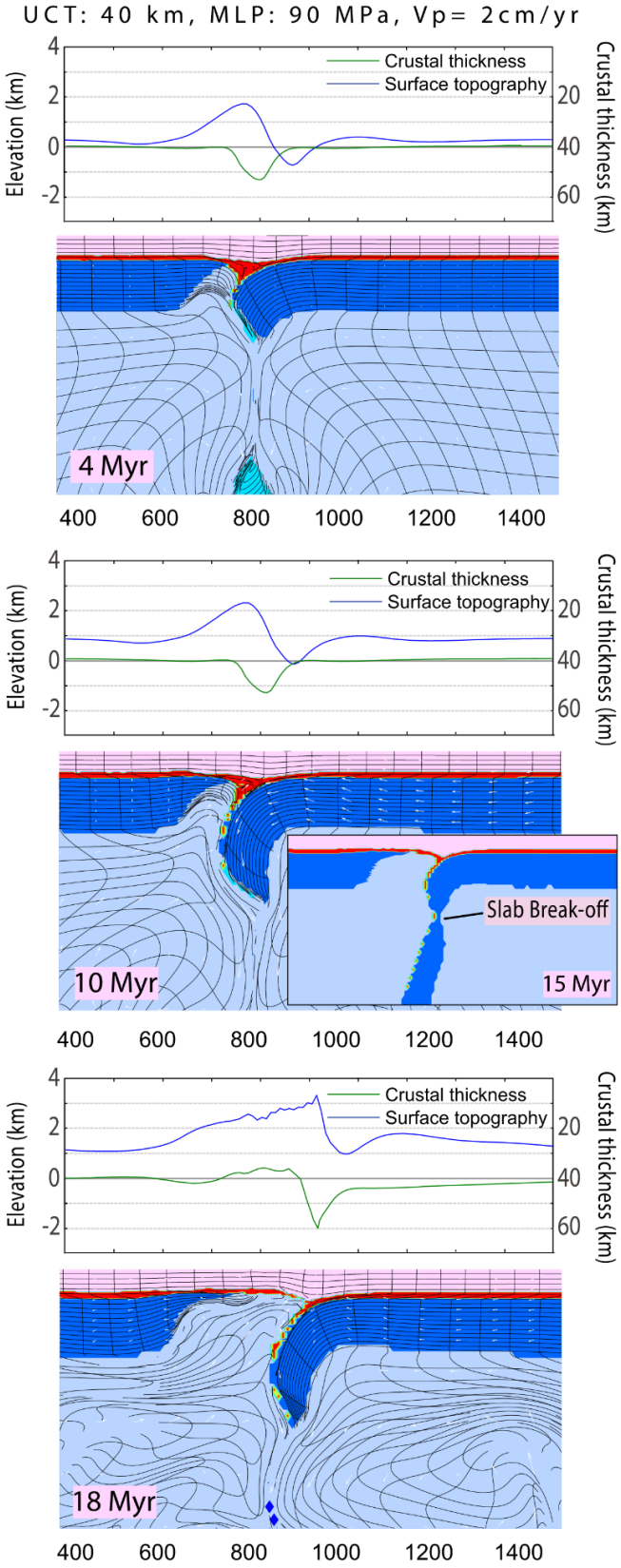

Figure 4.1 : The geodynamic evolution of the reference model and its crustal and topographical evolution in 18 Myr. The mantle lithosphere yield stress is 90 MPa, while the plate convergence rate is 2 cm/yr.

4.1.1 The effect of mantle lithosphere plasticity on slab break-off

Run-4162

In this model (Figure 4.3), a yield stress of 60 MPa has been used for the mantle lithosphere and a convergence rate of 2 cm/yr has imposed from the pro-side mantle lithosphere. The continental mantle lithosphere consists of 40 km in thick upper crust, 10 km in thick lower crust and 100 km in thick mantle lithosphere. The rheologies are determined as wet quartz in upper crust (Gleason and Tullis, 1996), felsic granulite in lower crust (Mackwell et al., 1998) and olivine in mantle lithosphere (Hirth and Kohlstedt, 1996). Reference densities of upper crust, lower crust and mantle lithosphere is 2840 kg/m3, 2990 kg/m3 and 3300 kg/m3, respectively.

At t=4 m.y. the denser oceanic part is disappeared due to its break-off. Following the break-off the topography is uplifted around 2 km over the asthenospheric column. A negative topography has been created by downward sinking pro-side mantle lithosphere, around 1,5 km. In this time, the crust has thickned up to 10 km based on imposed tensional force by the delaminated mantle lithosphere.

At t=10 m.y. the crust thinning has triggered by the rised hot asthenosphere and the topography is decreased over the asthenospheric column due to the load of the sinking mantle lithosphere. At t=18 m.y. the crust has thinned comparing to the crust at t=4 m.y. as around 12 km. This crustal thinning also evolves as a function of the delaminated mantle lithosphere as much as rised hot asthenosphere. In the models, the thickest crust has localized over the hinge location, while the thinnest crustal thickness has observed over the asthenospheric column. It is likely facilitates the crustal thinning that paddling of the pro-side mantle lithosphere through asthenosphere. The asthenospheric material resists to paddling movement of the mantle lithosphere and the lateral tensional force will be more effective on crustal thinning. When the crust is thinned, the rised asthenosphere can support to the topography positively due to decreases in the lithostatic pressure. At the t=18 m.y. the plateau-like, exceeding 3 km topography has been occured over the asthenospheric column, however; the slab break-off event was not observed. Therefore, this model not be responsible from the geodynamic evolution of the east Anatolian High Plateau.

Run-41122

In this model (Figure 4.2), we only imposed a convergence rate of 2 cm/yr from the right side of the box and plastic yield stress increased from 90 MPa to 120 MPa in comparison to the reference model.

The continental mantle lithosphere consists of 40 km in thick upper crust, 10 km in thick lower crust and 100 km in thick mantle lithosphere. The rheologies determined as wet quartz in upper crust (Gleason and Tullis, 1996), felsic granulite in lower crust (Mackwell et al., 1998) and olivine in mantle lithosphere (Hirth and Kohlstedt, 1996). Reference densities of upper crust, lower crust and mantle lithosphere is 2840 kg/m3, 2990 kg/m3 and 3300 kg/m3, respectively.

At time t=4 m.y. the oceanic part ruptures and/or breaks off from the pro-side mantle lithosphere and sinks. The sudden uplift is observed after the break off this denser part as mentioned in reference model. Note that this uplift only localized over the delamination hinge. At t=10 m.y. the pro-side mantle lithosphere is bent steeply into asthenosphere. This bending slab cause the thickens of crust above the hinge location. However, the crust has thinned ~2 km above the asthenospheric conduit in this time. At time t=18 m.y. the toe of pro-side mantle lithosphere has arrived to the bottom of the box. This boundry (660 km) is fixed hence do not permit to the penetration of slabs its own inside. Therefore, the vertical tensional force, which is affected on the pro-side mantle lithosphere has been diminished so that the break off event is not observed. In the reference model, the mantle lithosphere yield stress of 90 MPa was used and the break off observed in 15 Myr.

In the latest stage of the model (18 m.y.) the topography shows ~1 km decrease above the hinge location because the pro-side matle lithosphere undergoes to occur a load. In this time, the pro-side mantle lithosphere is bent as s-shaped and thickens at the dip levels.

In this model, we do not observed crustal thinning and the crustal thickness ranges from ~ 40 to 60 km. The maximum crustal thickness is observed above the delamination hinge location.

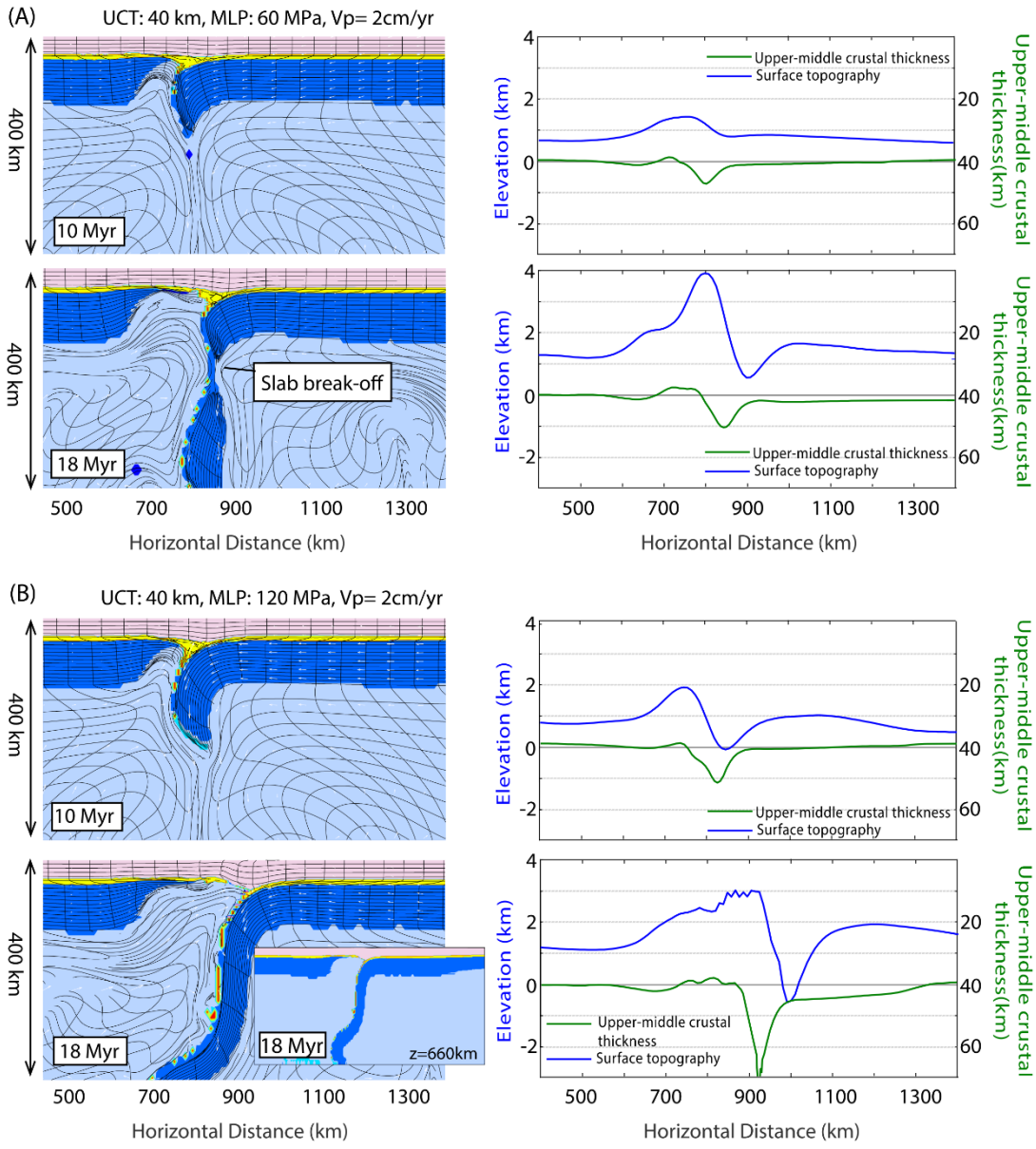

Figure 4.2 : The geodynamic evolution of Run-4162 and Run-41222 and its crustal and topographical evolution in 18 Myr.

4.1.2 The effect of plate convergence rate on post-delamination slab break-off

Run-4191

In this model (Figure 4.3), we imposed a convergence rate of 1 cm/yr from the right side of the box and plastic yield stress of 90 MPa is held fixed for pro-side mantle lithosphere. The continental mantle lithosphere consists of 40 km in thick upper crust, 10 km in thick lower crust and 100 km in thick mantle lithosphere. The rheologies are

determined as wet quartz in upper crust (Gleason and Tullis, 1996), felsic granulite in lower crust (Mackwell et al., 1998) and olivine in mantle lithosphere (Hirth and Kohlstedt, 1996). Reference densities of upper crust, lower crust and mantle lithosphere is 2840 kg/m3, 2990 kg/m3 and 3300 kg/m3, respectively.

At t=4 m.y. the oceanic part have triggered the delamination by pulling down the pro-side mantle lithosphere into asthenosphere (Figure 4.3). Thus, the pro-side mantle lithosphere is bent lowly and the crust has thickened 10 km over the delamination hinge. At t=10 m.y. the pro-side mantle lithosphere undergoes to peel away from the crust. The maximum topography is ~2 km, where the crust is absent from the mantle lithosphere and the thinnest. The topography is tend to be lower compare to the models, in which imposed higher convergence rates (2 to 5 cm/yr). At time t=18 m.y. the crustal thickness decreases ~ 2 km. This decrease at crustal thickness associated with the stretching of crust by the rised, relatively hotter asthenospheric column simultaneously decoupling of pro-side mantle lithosphere (Figure 4.3). The variations on crustal thickness is constrained with the delaminated area. At t=18 m.y. the pro-side mantle lithosphere is bent steeply and afterward its ruptured. The negative topography at t=4 m.y. has rebounded positively and the topography is exceed to 2 km.

Run-4193

In this model (Figure 4.3), we imposed a convergence rate of 3 cm/yr from the right side of the box and plastic yield stress of 90 MPa is used as in the reference model. The continental mantle lithosphere consists of 40 km in thick upper crust, 10 km in thick lower crust and 100 km in thick mantle lithosphere. The rheologies are determined as wet quartz in upper crust (Gleason and Tullis, 1996), felsic granulite in lower crust (Mackwell et al., 1998) and olivine in mantle lithosphere (Hirth and Kohlstedt, 1996). Reference densities of upper crust, lower crust and mantle lithosphere is 2840 kg/m^3, 2990 kg/m^3 and 3300 kg/m^3, respectively.

At time t=4 m.y., the crust has thicken ~10 km and the topography ~2 km uplifted above the hinge location. The oceanic part is detached earlier than reference model due to higher convergence rate. At t=10 m.y., the asthenospheric column is terminally closed and delamination event turn into a plate collision (Figure 4.3). In the models, in which imposed higher convergence rate (2 to 5 cm/yr) we observed a significant increase at crustal thickness and topography. However, these variations both on crust and topography characterized by the high convergence rate instead of asthenospheric

column. Since the asthenospheric column is not exist or widen enough to create topography (Figure 4.3). At time t=18 m.y. the crust thickened ~20 km in comparison to initiation time and it is not localized at immediate vicinity of delamination hinge. At time t=18 m.y. the topography exceeds 4 km, while crustal thickness exceeds 80 km. Such a high topography and thick crust is only observed in Tibetian Plateau in the earth. On the other hand, the break off is not observed in this model. The higher convergence rates (4 cm/yr) leds to rapid sinking of pro-side mantle lithosphere. Thus, pro-side mantle lithosphere could reach to the bottom of the box (660 km) without exposure much more tensional deformation.

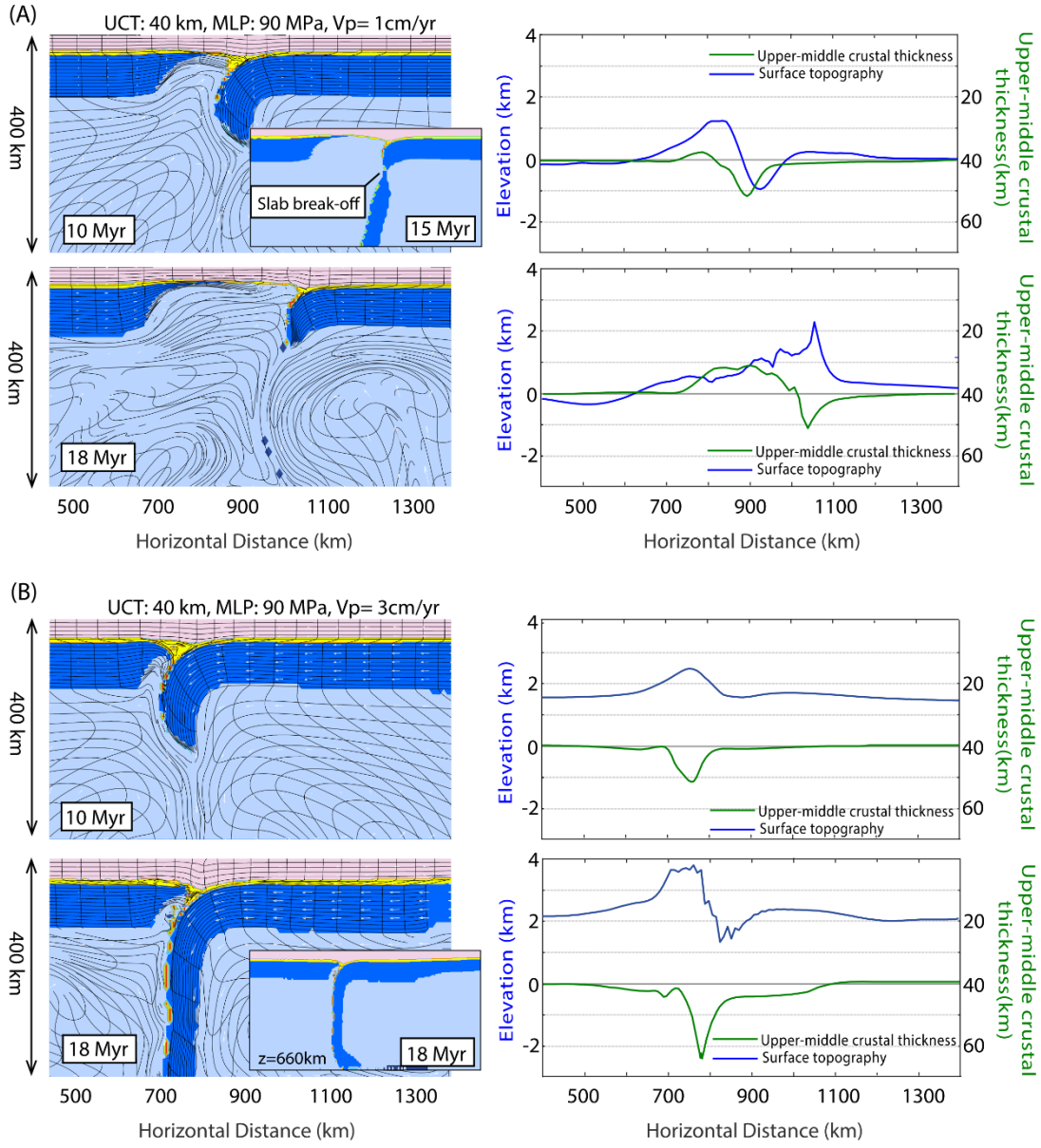

Figure 4.3 : The geodynamic evolution of the Run-4191 and Run-4193 and their crustal and topographical evolutions in 18 Myr.

4.2 The Evolution of Lithospheric Delamination in Oceanic Basement

Run OC72

In the preferred model (Figure 4.4), a convergence rate of 2 cm/yr imposed from the right margin of the lithosphere and plastic yield stress of 75 MPa is used for the mantle lithosphere.

The oceanic mantle lithosphere consists of 40 km in thick upper crust in diabase rheology, 10 km in thick lower crust (diabase) and 100 km in thick mantle lithosphere (olivine). Note that we scale down the effective viscousity of diabase upper crust by a factor of 0.1 to exhibit the properties of oceanic crust. Reference densities of upper crust, lower crust and mantle lithosphere is 2900 kg/m3, 3000 kg/m3 and 3300 kg/m3, respectively.

At t=4 m.y. the denser part is disappered due to its break off in the earlier time. The seperation of this part causes to pull down of the pro-side mantle lithosphere. Therefore, the crust has been thickned up to 5 km, while the topography has increased to ~1.7 km.. At t=10 m.y. delamination event being continued without break off event. The pro-side mantle lithosphere converging to the retro-side mantle lithosphere, therefore, the crust has shortened. Under the control of the convergence rate and occurrence of asthenospheric column, the topography has been uplifted around 2 km. In this experiment,. the break off of the pro-side mantle lithsophere is not observed until to the 15 m.y. Therefore, following to the break off a plateau-like topography is occured by the relaxiation in crustal level, in other word, with the rebounding of crust. At the same time, a negatie topography is yielded due to ongoing slab movement into asthenosphere. The dipping angle of this descenting slab also specify that the location of the negative topography. In general, negative topography is observed in the right side of the thickest point of crust.

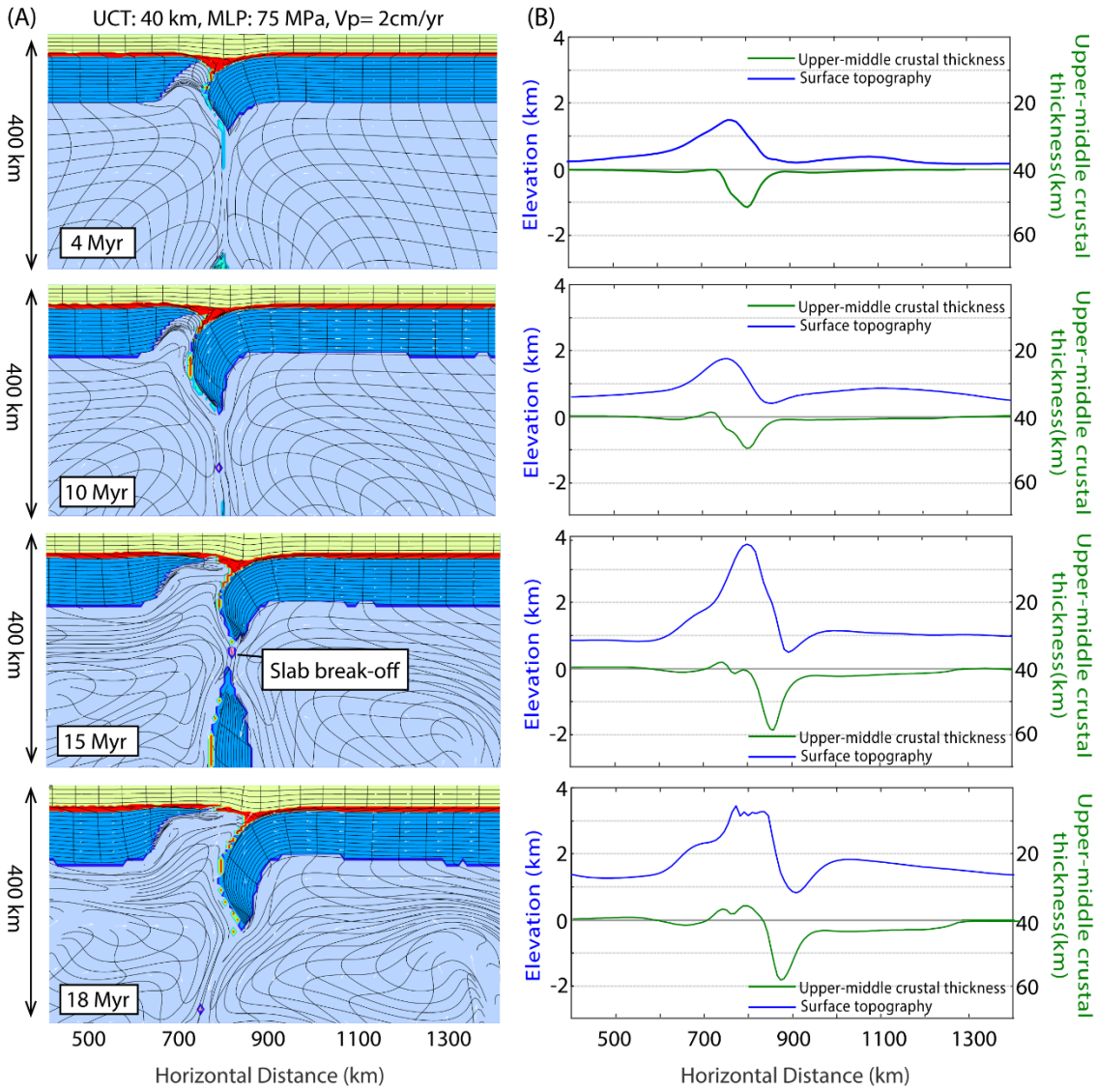

Figure 4.4 : The geodynamic evolution of the Run-OC72 and its crustal and topographical evolution in 18 Myr.

Run- OC92

Yield stress of 90 MPa has been used for the mantle lithosphere and a convergence rate of 2 cm/yr has imposed from the pro-side mantle lithosphere (Figure 4.5). At t=4 m.y. the denser part is pulled down the pro-side mantle lithosphere. Therefore, the crust has been thickned up to 5 km, while the topography is uplifted around 2 km. At t= 10 m.y., the pro-side mantle lithosphere is steepenned, while about 2 km topograhy is formed. In hinge location, the crustal thickness thickened more than 10 km due to steeply being sinked pro-side mantle lithosphere. At t= 18 m.y., the slab break-off event is not observed yet. However, there is a anormal extensional deformation at ~300 km-depth on slab. In further stages, roughly in 2 myrs. the break-off event will be occur. In this experiment, the crust is thickened ~30 km compare to the initial thickness (40 km), while -1 km negative topography is yielded in the back side of the delamination hinge location. These abnormal variations on crustal thickness and topography resultants of the pro-side mantle lithosphere is that being contunied to sink.

Run OC62

Yield stress of 60 MPa has been used for the mantle lithosphere and a convergence rate of 2 cm/yr has imposed from the pro-side mantle lithosphere (Figure 4.5). At t= 4 m.y, the break off of the denser part has been triggered the deformation of the toe of the pro-side mantle lithosphere by viscously creeping into asthenosphere. At t=10 m.y. delamination event being continued without break off event. The pro-side mantle lithosphere converging to the retro-side mantle lithosphere, therefore, the crust has shortened. Owing to the convergence and dynamic support of rised asthenosphere, the topography has been uplifted exceeds 3 km.. At t=18 m.y.,. the pro-side mantle lithosphere is ruptured and being sinked in to asthenosphere. Hence the topography is rapidly increased (~4 km) as a result of the replacing of the descenting slab via hot asthenosphere.

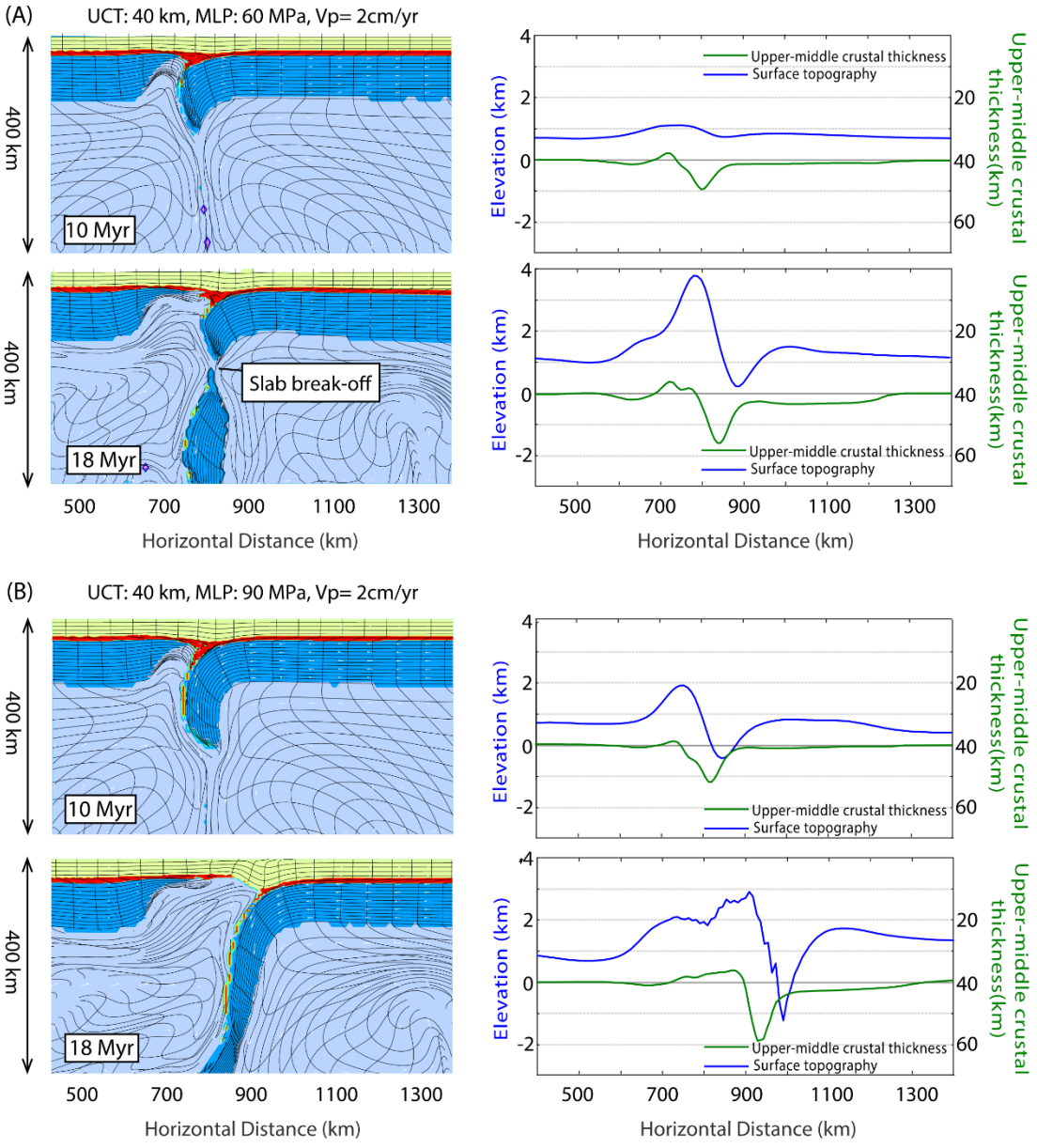

Figure 4.5 : The geodynamic evolution of Run-OC62 and Run-OC92 and their crustal and topographical evolution in 18 Myr.

Run OC71

Convergence rate of 1 cm.yr^{-1} is imposed from the right side of the lithosphere and plastic yield stress of 75 MPa is used for the mantle lithosphere (Figure 4.6). At t= 10 m.y., the topography is obviously higher than in RUN-OC70 since the applied convergence. The pro-side mantle lithosphere breaks-off at t=15 m.y. At t= 18m.y., the crust is thiner than in RUN-OC70 although to the imposed convergence rate. Thus, syn-convergent extenison is observed in this experiment. The maximum elevation is around 3 km and corresponds to over the hinge location. Therefore, it can be say that the elevation is also highly supported by crustal contraction.

Run OC73

Convergence rate of 3 cm.yr^{-1} is imposed from the right side of the lithosphere and plastic yield stress of 75 MPa is used for the mantle lithosphere (Figure 4.6). Unlike the continental basement experiment in same plate convergence rate (3cm.yr^{-1}), the slab break-off event is observed in this experiment at t=18 m.y. Also an avaraged ~3 km topography occured. The crust is extremely thickned due to being sinking mantle lithosphere as localized over the delamination hinge point. The topography is increased along the whole of the crustal layer since the high plate convergence.

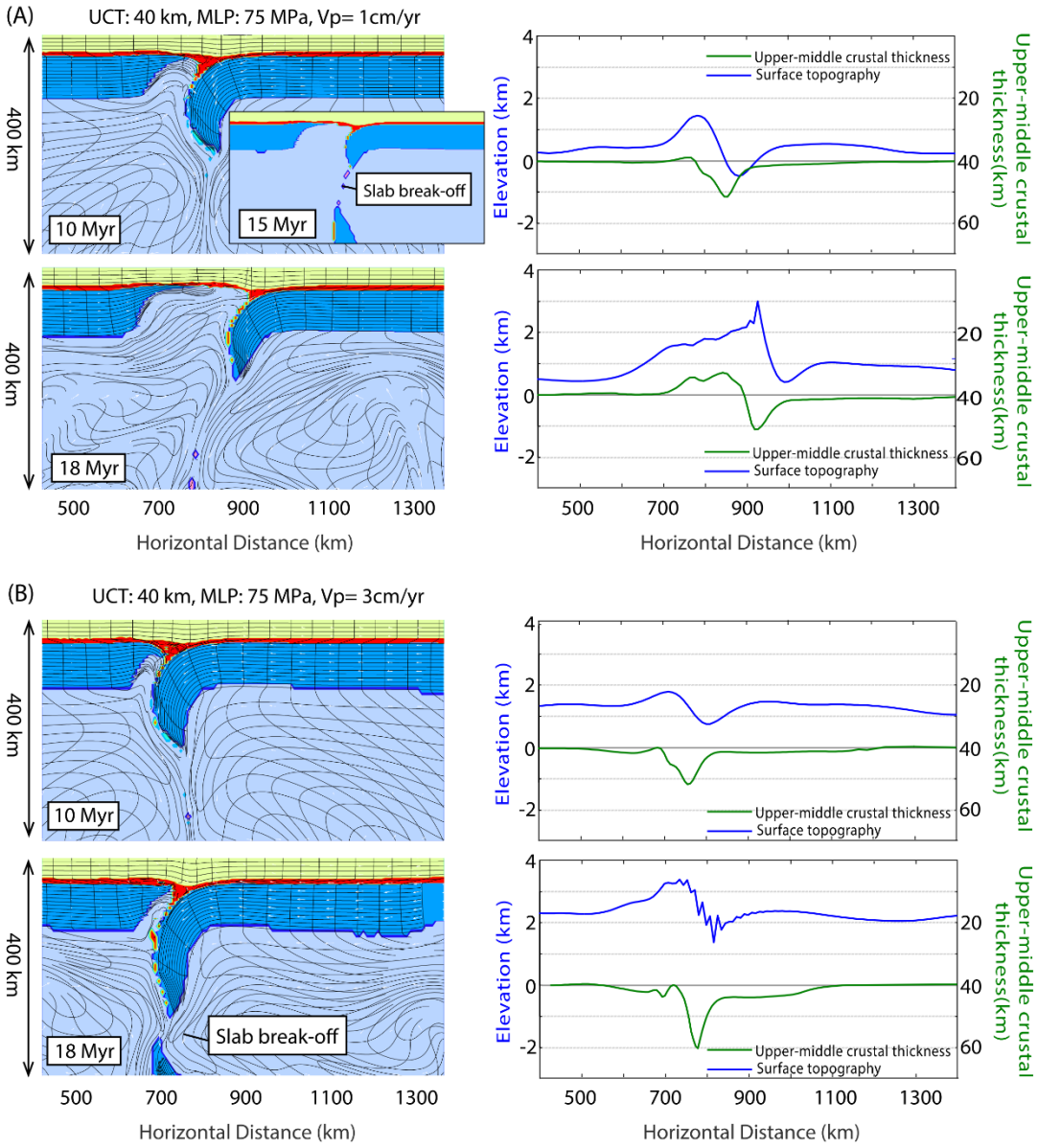

Figure 4.6 : The geodynamic evolution of Run-OC71 and Run-OC73 and their crustal and topographical evolution in 18 Myr.

5. CONCLUSIONS

5.1 Topography and Crustal Thickness Observations and the Ability of Delamination at Plateau Growth

Throughout the experiments, the topography evolved as depending on: (1) upper crustal thikness; (2) plate convergence rate; (3) the width of asthenospheric column. Increasing of upper crustal thickness has a negative effect on plateau growth via delamination. The uplift only take place if lithostatic pressure at the base of the crust is higher than the static pressure of rised hot asthenosphere (Bird, 1979). However, in some model, the asthenospheric column is not widen enough to create dynamic topography due to high convergence rates (3 to 5 cm/yr). In this case, the delamination event turned into plate collision and the asthenospheric column is totally disappeared. Therefore, the topography is created by crustal shortening owing to high convergence rate. In the models, we also observed rebounding of topography following the slab break off in short time scale relatively. The topography rebounded ~4 km in 4 Myr.

In general, crustal thickness decreased over the delaminated area due to stretching of crust by being rised asthenospheric column. However, the crustal thickness is always maximum over the delamination hinge and this localized thick crust migrates with hinge location excluding the models, in which imposed high convergence rate (3 to 5 cm/yr).

To better understanding of the ability of delamination at the plateau growth, the upper crustal thickness has been changed from 40 km to 30km. The model's results has been compared in Figure 5.2. The Figure 5.1 demonstrates the connection between mantle lithosphere yield stress, plate convergence rate and avarage uplift amount over the plateau gap or asthenospheric column for continental basement models. According to the Figure 5.1, the avarage uplift amount over the asthenospheric column is changed mostly based on upper crustal thickness and plate convergence rate. There is no effect of the mantle lithosphere yield stress on the topography. When the upper crustal

thickness is decreased (Figure 5.5) the topography is increased due to decreased at the lithostatic pressure.

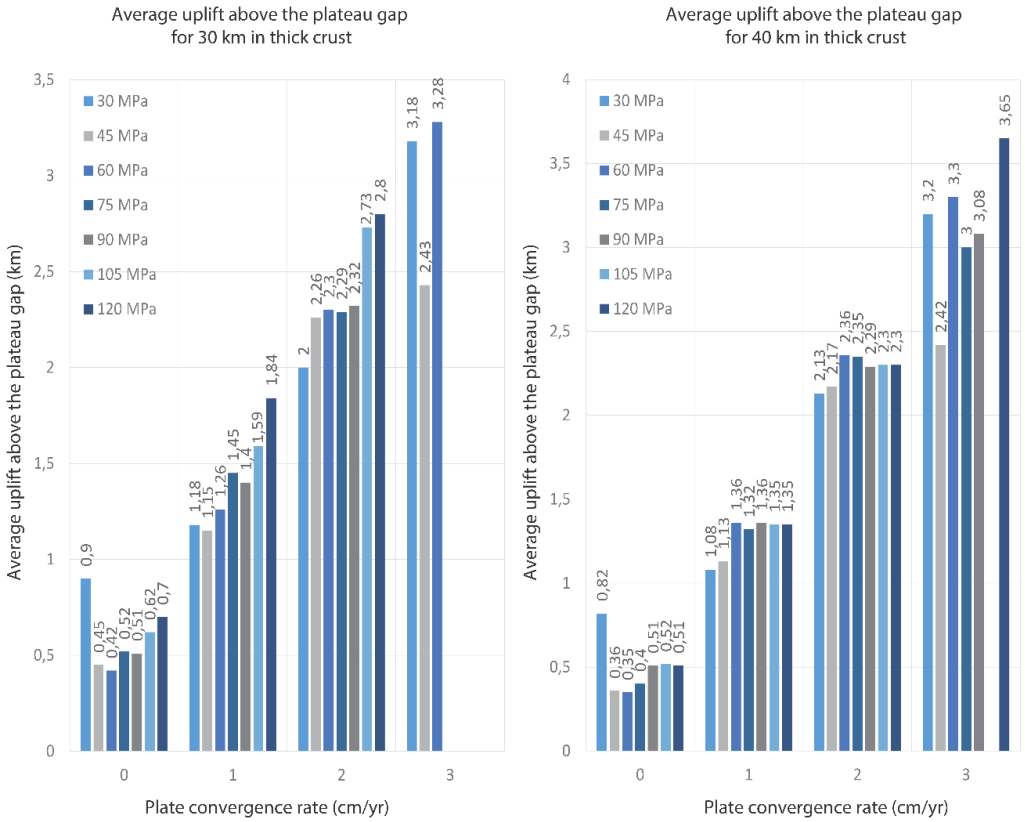

Figure 5.1 : The plot shows the avarage uplift amounts in the post-delamination break-off cases. 30 km and 40 km in thick upper crust is used and the values over the bars shows the amount of uplifted topography in 18 Myr.

5.2 Comparision of Model Result with Observed Anomalies

The experimental results of the reference models pertaining to the RUN-4192 (continental) and RUN-OC72 have been compared with the observed data belong to the east Anatolian Plateau in Figure 11 and Table 3.1 RUN-4192 the avarage uplift amount over the asthenopsheric column is 2.3 km, while 2.48 km in RUN-OC72 within 18 Myrs. The approximated asthenospheric column width of RUN-4192 and RUN-OC72 are 328 km and 264 km, respectively. The witdh of the asthenospheric column is narrower in RUN-OC72. Hence, the crustal shorthening is more dominate than the dynamic support of asthenosphere and so that the avarage uplift amount is higher. Note that the avarage uplift amounts are only include area of the over the mantle lithosphere-free area.

The crustal thickness profiles obtained from the experiments are not coherent with the observed data along the east Anatolian Plateau. The crust has thickenning to the north and ranging between 38 to 50 km in east Anatolia (Zor et al., 2003). The big differences between the observed and the modeled crustal thickness data may be arised from the lacking of the surficial and near-surfical deformations such as faulting. The another reason is that the time of the slab break-off. During the paddling movement of slab, the crust being thickened as localized over the hinge location due to the affecting vertical tensional forces until to the detacthment of the sinking delaminated slab. This is because the excessive thickenning in the crust at the delamination hinge location.

The topographic profiles belong to both of two reference model are quite consist with the topography along the east Anatolia. The location of the subsidence is also perfectly compatible. In the experiments, the thickest crustal point is always retreated together with the delamination hinge location, while the subsidence occurs in the south of the thickest crustal point.

A similiar case has been observed in the east Anatolian Plateau (see Figure 5.2). The observed data shows that topography is decreased in Muş basin and the crustal thickness is increased to 48 km in the north of Muş basin. The reduction in the topography may be related with the remain part of the detacthed and being sinked Arabian mantle lithosphere. Gans et al. (2009) have shown that high Pn-velocity beneath the Bitlis suture. This high velocity may be occured as a result of the remain part of being sinked Arabian mantle lithosphere. In this case, the formation of Muş basin and observed topography would be explained well. The remain mantle lithosphere part may be responsible from the decreasing at the topography in Muş basin.

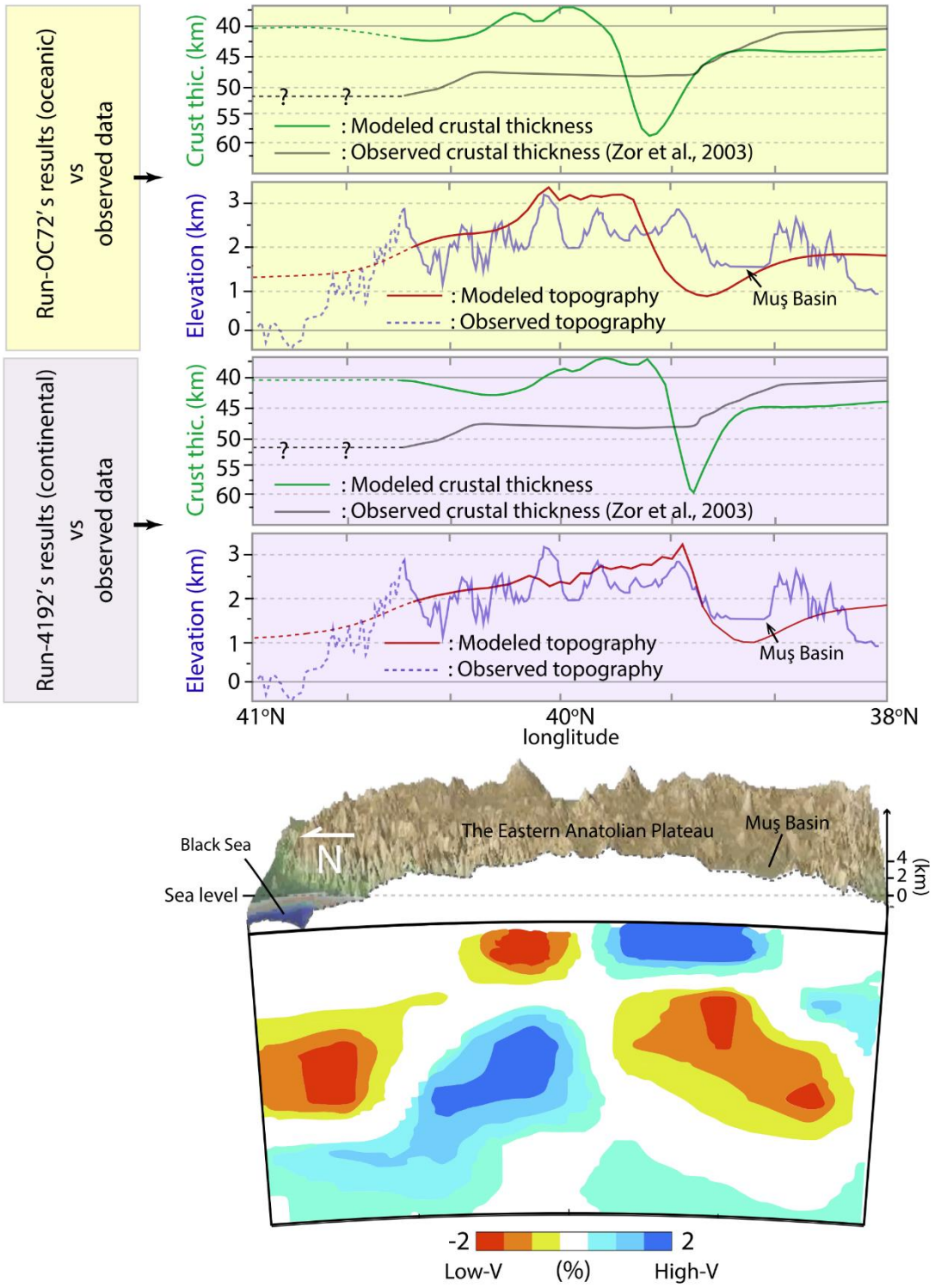

Figure 5.2 : Comparison of model results with observed data in east Anatolia. The tomographic cross section modified from Lei & Zhao, 2007.

5.3 Occurrence of Delamination in Continental and Oceanic Basement

We conducted our lithospheric delamination models for both continental and oceanic basement. Former geological studies were suggested that the east Anatolian High Plateau basement is oceanic and the uplift formed as domal shape over the accreation-prism. However, current studies suggested that the basement of the east Anatolian Plateau might be continental, according to the distrubution of ophiolites and ophiolitic melanges.

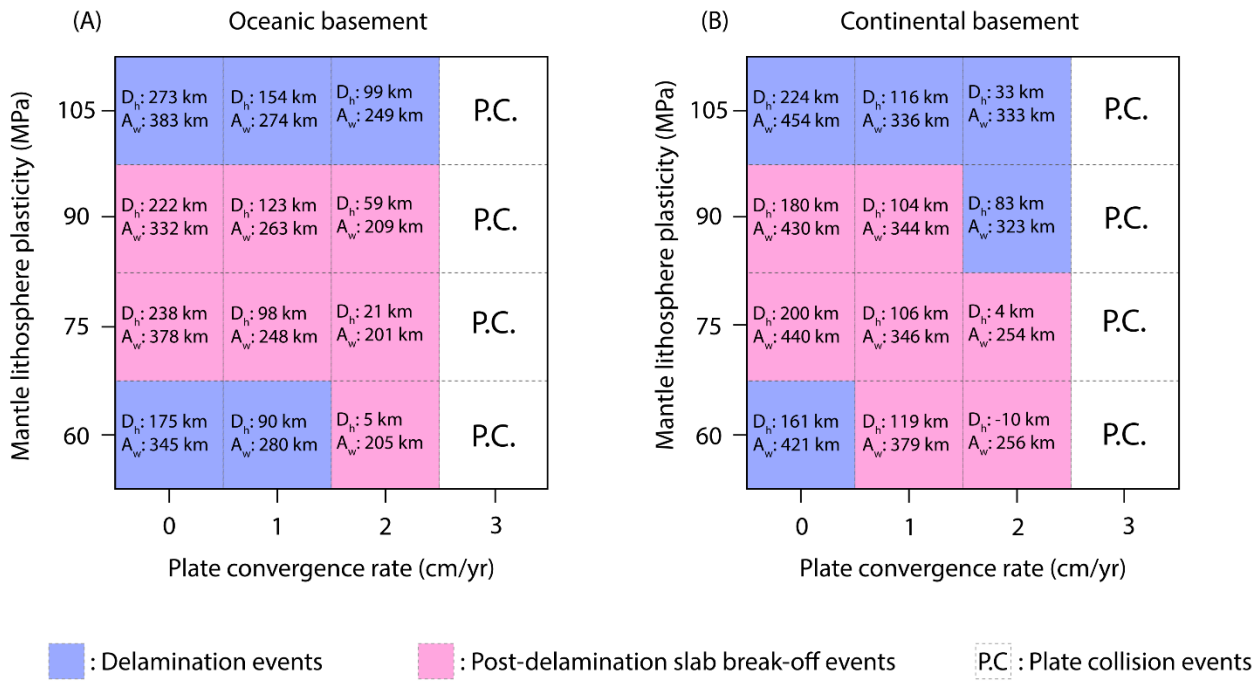

Figure 5.3 : The plot shows the delamination hinge migration (Dh) and asthenospheric width (Aw) amounts for continental and oceanic basements.

In the continental basement models, we have been used a 100 km-thick mantle lithosphere for pro-side mantle lithosphere and quartz rheology in upper while in the oceanic basement models we used a 80 km-thick mantle lithosphere and diabase rheology in upper crust. Note that we scale down the effective viscousity of diabase upper crust by a factor of 0.2 to exhibit the properties of oceanic crust. Model results show that there is a noticiable difference in lateral delamination speed between oceanic and continental basement models. In oceanic basement models, the mantle lithosphere thickness 20 km decreased, therefore, the pro-side mantle lithospere could not delaminate enough to create plateau. However, in continental basement models, the pro-side mantle lithosphere could be delaminate easier than the oceanic models, and we observed the plateau-like topography after 18 Myr. The mantle lithosphere tickness may be main effect on the controlling lateral delamination speed hence the width of asthenospheric column instead of upper crustal rheology. The fact that upper crustal rheology is a controller parameter of the rising of topography owing to its own lithostatic pressure. In higher densities of upper crustal rheology the topography cannot uplift so that the plateau is not formed. Figure 5.3 shows the differences in delamination hinge migration for both oceanic and continental basement models. In this figure, it is clearly seen that the delamination hinge migration amounts higher in continental basement.

5.4 Mantle Lithosphere Plasticity and Convergence Rate vs Slab Break-off

The fate of the pro-plate develops mainly based on slab buoyancy, mantle adiabat, frictional stress and mineral composition of interacted material bodies (Billen, 2008).

It is well known that the continental rocks are more buoyant and less dence than oceanic rocks (Turcotte, 1987). Therefore, the peeling process slows down after introducing of continental rocks into asthenosphere. In fact, this may be reason for detachment of an oceanic lithosphere from a continental. Regard et al (2008) based on laboratory experiments reported that the tensional force maximized at the merge point of continental and oceanic lithosphere due to higher speeds at the dip-part of oceanic slab than imposed by convergence rate. In other words, resistance force to sink of softer rocks directly moderates the lateral speed of subduction/delamination as much as detacthment of oceanic slab. As a concept, it is suggested that the colder hence more dense lithospheric mantle susceptible to subduction due to its negative buoyancy.

Cloos (1993) reported that even the youngest (~10 m.y.) oceanic lithosphere that tend to subduct and this took place easier than continental subduction. Since the during an oceanic subduction the density of crust constantly increases based on by metamorphosing of basalt/gabbro in upper crust into denser amphiobolite and eclogite. This metamorphosis in the subduction zones preserve the negative buoyancy of being subducted slab. However, in continental subduction the crust mainly build up by granitic therefore the buried less dense crustal material than asthenosphere causes to the development of resistance forces to subduction (Cloos, 1993).

In this section of the experimental series, in order to investigate the sensivity of slab break-off we systematically change that the parameters of mantle lithosphere plasticity and convergence rate. A broad-range of plasticity values (30, 45, 60, 75, 90, 105, 120 MPa) and convergence rate (0 to 5 cm/yr) has been imposed.

Our model results show that the slab break-off is occurred only in a certain range of convergence rate (0 to 2cm/yr) regardless of mantle lithosphere plasticity (Figure 10). In contrast, the higher convergence rates (3 to 5 cm/yr) promotes rapid bending and dipping of the delaminated mantle lithosphere. Therefore, the mantle lithosphere can reach to the lower mantle (660 km) in 15 Myr. This prevents further sinking and counteracting much more tensional deformation of slab, the slab-break off event has not been observed at the models in which imposed higher convergence rates (3 to 5cm/yr). Note that the slab penetration is not permitted through a fixed boundry in depth of 660 km.

On the other hand, we found that mantle lithosphere plasticity concludes that how the mantle lithosphere will deform. For example, Run-4132 shows the evolution of delamination, in which a plastic yield stress of 30 MPa is used for the mantle lithosphere and plate convergence rate is not imposed. In the Run-4132, failure of the mantle lithosphere occurs in ductile mode. However, by increasing of plastic yield stress the mantle lithosphere becomes stronger, as shown in Figure 3b, plastic yield stress of 120 MPa is used.

Overall, the realization probability of the slab break-off is directly proportional with (1) slab pull force arise from unceasingly ongoing peeling of mantle lithosphere; (2) inversely proportional with convergence rate and (3) mantle lithosphere plasticity.

REFERENCES

Angus, D. A., Wilson, D. C., Sandvol, E., & Ni, J. F. (2006). Lithospheric structure of the Arabian and Eurasian collision zone in eastern Turkey from S-wave receiver functions. Geophysical Journal International, 166(3), 1335-1346.

Artemieva, I. (2011). The lithosphere: An interdisciplinary approach. Cambridge University Press.

Ates, A., Bilim, F., & Buyuksarac, A. (2005). Curie point depth investigation of Central Anatolia, Turkey. pure and applied geophysics, 162(2), 357-371.

Aydın, İ., Karat, H. İ., & Koçak, A. (2005). Curie-point depth map of Turkey.Geophysical Journal International, 162(2), 633-640.

Barazangi, M., Sandvol, E., & Seber, D. (2006). Structure and tectonic evolution of the Anatolian plateau in eastern Turkey. Geological Society of America Special Papers, 409, 463-473.

Billen, M. I. (2008). Modeling the dynamics of subducting slabs. Annu. Rev. Earth Planet. Sci., 36, 325-356.

Bird, P. (1979). Continental delamination and the Colorado Plateau. Journal of Geophysical Research: Solid Earth, 84(B13), 7561-7571.

Bird, P. (1991). Lateral extrusion of lower crust from under high topography in the isostatic limit. Journal of Geophysical Research: Solid Earth, 96(B6), 10275-10286.

Bozkurt, E. (2001). Neotectonics of Turkey–a synthesis. Geodinamica acta,14(1-3), 3-30.

Burov, E. B. (2011). Rheology and strength of the lithosphere. Marine and Petroleum Geology, 28(8), 1402-1443.

Chapman, D. S., Bartlett, M. G., & Harris, R. N. (2004). Comment on "Ground vs. surface air temperature trends: Implications for borehole surface temperature reconstructions" by ME Mann and G. Schmidt. Geophysical research letters, 31(7).

Cloos, M. (1993). Lithospheric buoyancy and collisional orogenesis: Subduction of oceanic plateaus, continental margins, island arcs, spreading ridges, and seamounts. Geological Society of America Bulletin, 105(6), 715-737.

Demirtaşlı, E., & Pisoni, C. (1965). The geology of Ahlat–Adilcevaz area (north of Lake Van). MTA Bull, 61, 23-36.

Duretz, T., & Gerya, T. V. (2013). Slab detachment during continental collision: Influence of crustal rheology and interaction with lithospheric delamination.Tectonophysics, 602, 124-140.

Fullsack, P. (1995). An arbitrary Lagrangian-Eulerian formulation for creeping flows and its application in tectonic models. Geophysical Journal International,120(1), 1-23.

Gelati, R. O. M. A. N. O. (1975). Miocene marine sequence from Lake Van, eastern Turkey. Riv. Ital. Paleontol. Stratigr, 81, 477-490.

Gerya, T. V., Maresch, W. V., Willner, A. P., Van Reenen, D. D., & Smit, C. A. (2001). Inherent gravitational instability of thickened continental crust with regionally developed low-to medium-pressure granulite facies metamorphism.Earth and Planetary Science Letters, 190(3), 221-235.

Gleason, G. C., & Tullis, J. (1995). A flow law for dislocation creep of quartz aggregates determined with the molten salt cell. Tectonophysics, 247(1), 1-23.

Gök, R., Pasyanos, M. E., & Zor, E. (2007). Lithospheric structure of the continent—continent collision zone: eastern Turkey. Geophysical Journal International, 169(3), 1079-1088.

Göğüş, O. H., & Pysklywec, R. N. (2008). Mantle lithosphere delamination driving plateau uplift and synconvergent extension in eastern Anatolia.Geology, 36(9), 723-726.

Hess, H. H. (1962). History of ocean basins. Petrologic studies, 4, 599-620.

Hirth, G., & Kohlstedt, D. L. (1996). Water in the oceanic upper mantle: implications for rheology, melt extraction and the evolution of the lithosphere.Earth and Planetary Science Letters, 144(1), 93-108.

Kay, S. M. (1993). Fundamentals of statistical signal processing, volume I: estimation theory.

Keskin, M. (2003). Magma generation by slab steepening and breakoff beneath a subduction-accretion complex: An alternative model for collision-related volcanism in Eastern Anatolia, Turkey. Geophysical Research Letters, 30(24).

Keskin, M. (2007). Eastern Anatolia: a hotspot in a collision zone without a mantle plume. Geological Society of America Special Papers, 430, 693-722.

Kirby, S. H., & Kronenberg, A. K. (1987). Rheology of the lithosphere: selected topics. Reviews of Geophysics, 25(6), 1219-1244.

Lei, J., & Zhao, D. (2007). Teleseismic evidence for a break-off subducting slab under Eastern Turkey. Earth and Planetary Science Letters, 257(1), 14-28.

Magni, V., Faccenna, C., Hunen, J., & Funiciello, F. (2013). Delamination vs. break-off: the fate of continental collision. Geophysical Research Letters, 40(2), 285-289.

Mackwell, S. J., Zimmerman, M. E., & Kohlstedt, D. L. (1998). High-temperature deformation of dry diabase with application to tectonics on Venus.Journal of Geophysical Research: Solid Earth, 103(B1), 975-984.

Morency, C., & Doin, M. P. (2004). Numerical simulations of the mantle lithosphere delamination. Journal of Geophysical Research: Solid Earth,109(B3).

Oberhänsli, R., Candan, O., Bousquet, R., Rimmele, G., Okay, A., & Goff, J. (2010). Alpine high pressure evolution of the eastern Bitlis complex, SE Turkey. Geological Society, London, Special Publications, 340(1), 461-483.

Özacar, A. A., Gilbert, H., & Zandt, G. (2008). Upper mantle discontinuity structure beneath East Anatolian Plateau (Turkey) from receiver functions.Earth and Planetary Science Letters, 269(3), 427-435.

Özacar, A. A., Zandt, G., Gilbert, H., & Beck, S. L. (2010). Seismic images of crustal variations beneath the East Anatolian Plateau (Turkey) from teleseismic receiver functions. Geological Society, London, Special Publications, 340(1), 485-496.

Pamukçu, O. Akç›¤, Z. Hisarl›, M., Tosun, S. 2014. Curie point depths and heat flow of Eastern Anatolia (Turkey). Energy Sources, Part A: Recovery, Utilization, and Environmental Effects, 24, 2699-2706.

Pearce, J. A., Bender, J. F., De Long, S. E., Kidd, W. S. F., Low, P. J., Güner, Y., ... & Mitchell, J. G. (1990). Genesis of collision volcanism in Eastern Anatolia, Turkey. Journal of Volcanology and Geothermal Research, 44(1), 189-229.

Ranalli, G. (1995). Rheology of the Earth. Springer Science & Business Media.

Regard, V., Faccenna, C., Bellier, O., & Martinod, J. (2008). Laboratory experiments of slab break-off and slab dip reversal: insight into the Alpine Oligocene reorganization. Terra Nova, 20(4), 267-273.

Piromallo, C., & Morelli, A. (2003). P wave tomography of the mantle under the Alpine-Mediterranean area. Journal of Geophysical Research: Solid Earth,108(B2).

Schildgen, T. F., Yıldırım, C., Cosentino, D., & Strecker, M. R. (2014). Linking slab break-off, Hellenic trench retreat, and uplift of the Central and Eastern Anatolian plateaus. Earth-Science Reviews, 128, 147-168.

Stern, R. J. (2002). Subduction zones. Reviews of geophysics, 40(4).

Şengör, A. M. C., Özeren, S., Genç, T., & Zor, E. (2003). East Anatolian high plateau as a mantle-supported, north-south shortened domal structure.Geophysical Research Letters, 30(24).

Şengör, A. C., Özeren, M. S., Keskin, M., Sakınç, M., Özbakır, A. D., & Kayan, I. (2008). Eastern Turkish high plateau as a small Turkic-type orogen: Implications for post-collisional crust-forming processes in Turkic-type orogens.Earth-Science Reviews, 90(1), 1-48.

Topuz, G., Okay, A. I., Altherr, R., Schwarz, W. H., Sunal, G., & Altınkaynak, L. (2014). Triassic warm subduction in northeast Turkey: Evidence from the Ağvanis metamorphic rocks. Island Arc, 23(3), 181-205.

Turcotte, D. L. (1987). Rheology of the oceanic and continental lithosphere.Composition, Structure and Dynamics of the Lithosphere-Asthenosphere System, 61-67.4.

Wegener, Alfred. (1966). The origin of continents and oceans. Courier Corporation.

Wyche, S., Nelson, D. R., & Riganti, A. (2004). 4350–3130 Ma detrital zircons in the Southern Cross Granite–Greenstone Terrane, Western Australia: implications for the early evolution of the Yilgarn Craton. Australian journal of Earth sciences, 51(1), 31-45.

Van der Pluijm, Ben, and Stephen Marshak. "Earth structure." vine 34 (2004): 429-432.

Yilmaz, A., Yilmaz, H., Kaya, C., & Boztug, D. (2010). The nature of the crustal structure of the Eastern Anatolian Plateau, Turkey. Geodinamica Acta,23(4), 167-183.

Yılmaz, Y., Güner, Y., & Şaroğlu, F. (1998). Geology of the Quaternary volcanic centres of the East Anatolia. Journal of volcanology and geothermal research,85(1), 173-210.

Yilmaz, Y., Şaroğlu, F., & Güner, Y. (1987). Initiation of the neomagmatism in East Anatolia. Tectonophysics, 134(1), 177-199.

Zor, E., Sandvol, E., Gürbüz, C., Türkelli, N., Seber, D., & Barazangi, M. (2003). The crustal structure of the East Anatolian plateau (Turkey) from receiver functions. Geophysical Research Letters, 30(24).

Zor, E. (2008). Tomographic evidence of slab detachment beneath eastern Turkey and the Caucasus. Geophysical Journal International, 175(3), 1273-1282.

APPENDICES

APPENDIX A: Tables

Table A.1 : Models' results table

Model No	Mantle lithosphere plasticity (Mpa)	Plate velocity (cm/yr)	Hinge migration amount (km)	Coordinates of PMG	Average uplift above the plateau gap (km)	The width of plateau making gap (km)	Rheology of upper crust	Rheology of lower crust
4130	30	0	480	550-1380	0,85	830	Quartz	Felsic Granulite
4131	30	1	360	550-1260	1,13	710	Quartz	Felsic Granulite
4132	30	2	170	590-1070	2,24	480	Quartz	Felsic Granulite
4133	30	3	-20	590-880	3,65	290	Quartz	Felsic Granulite
4134	30	4	X	X	X	X	Quartz	Felsic Granulite
4135	30	5	X	X	X	X	Quartz	Felsic Granulite
4140	45	0	270	650-1170	0.45	520	Quartz	Felsic Granulite
4141	45	1	120	680-1020	1,25	340	Quartz	Felsic Granulite
4142	45	2	-30	660-870	2.35	110	Quartz	Felsic Granulite
4143	45	3	-120	X	X	X	Quartz	Felsic Granulite
4144	45	4	X	X	X	X	Quartz	Felsic Granulite
4145	45	5	X	X	X	X	Quartz	Felsic Granulite
4160	60	0	190	730-1090	0.47	360	Quartz	Felsic Granulite
4161	60	1	80	980-710	1.52	270	Quartz	Felsic Granulite
4162	60	2	-10	700-890	2.82	190	Quartz	Felsic Granulite
4163	60	3	-100	X	X	X	Quartz	Felsic Granulite
4164	60	4	X	X	X	X	Quartz	Felsic Granulite
4165	60	5	X	X	X	X	Quartz	Felsic Granulite
4170	75	0	230	760-1130	0.55	370	Quartz	Felsic Granulite
4171	75	1	X	X	X	X	Quartz	Felsic Granulite
4172	75	2	0	720-900	2.68	180	Quartz	Felsic Granulite
4173	75	3	-90	X	X	X	Quartz	Felsic Granulite
4174	75	4	X	X	X	X	Quartz	Felsic Granulite

Table A.1 (continued): Delamination hinge migration amounts

4175	75	5	X	X	X	X	Quartz	Felsic Granulite
4190	90	0	200	790-1100	0.64	310	Quartz	Felsic Granulite
4191	90	1	100	760-1000	1.63	240	Quartz	Felsic Granulite
4192	90	2	50	950-750	2.57	200	Quartz	Felsic Granulite
4193	90	3	-80	X	X	X	Quartz	Felsic Granulite
4194	90	4	X	X	X	X	Quartz	Felsic Granulite
4195	90	5	X	X	X	X	Quartz	Felsic Granulite
41100	105	0	260	790-1160	0.65	370	Quartz	Felsic Granulite
41101	105	1	140	780-1040	1.57	260	Quartz	Felsic Granulite
41102	105	2	90	750-990	2.54	240	Quartz	Felsic Granulite
41103	105	3	-100	x	x	x	Quartz	Felsic Granulite
41104	105	4	x	x	x	x	Quartz	Felsic Granulite
41105	105	5	x	x	x	x	Quartz	Felsic Granulite
41120	120	0	240	780-1140	0.61	360	Quartz	Felsic Granulite
41121	120	1	120	800-1020	1.68	220	Quartz	Felsic Granulite
41122	120	2	70	760-970	2.62	210	Quartz	Felsic Granulite
41123	120	3	-100	x	x	x	Quartz	Felsic Granulite
41124	120	4	x	x	x	x	Quartz	Felsic Granulite
41125	120	5	x	x	x	x	Granite	Felsic Granulite
4160-o	60	0	60	730-1350	0.40	620	Granite	Felsic Granulite
4161-o	60	1	-10	720-1350	0.83	630?	Granite	Felsic Granulite
4162-o	60	2	-120	770-1210	1.65	440	Granite	Felsic Granulite
4163-o	60	3	X	x	x	x	Granite	Felsic Granulite
4170-o	75	0	22 or 60	770-1500	0.34	730	Granite	Felsic Granulite
4171-G	75	1	zz	750-1330	0.80	580	Granite	Felsic Granulite
4172-G	75	2	290	800-119	1.71	390	Granite	Felsic Granulite
4173-G	75	3	190	800-1090	2.51	290	Granite	Felsic Granulite
Total								50

O. Caner Memis, MSc student
İstanbul Technical University

Eurasia Institute of Earth Sciences Istanbul Technical University Maslak, 34469, Istanbul, Turkey. Phone: +90 544 497 17 17
E-mail: canermemis@yahoo.com

Education

2008-2013 : Çanakkale OnSekiz Mart University
BSc in Geopgysical Engineering
Thesis topic: "Liquefaction of ground and examination of its possibility".
Final Grade: 2.28/4

2014-2016 : İstanbul Technical University
MSc in Geodynamics
Thesis topic: " Geodynamic modeling the styles of lithospheric delamination with application to the Eastern Anatolia".

Conferences/Presentations

1. " Geodynamic mechanisms of plateau uplift and strain distribution in Eastern Anatolia", Poster in EGU/Vienna, April/2015.

2. " Modeling the evolution of loss of subdtucting plate under the Eastern Anatolia by testing various rheological and compositional properties", Poster in AGU/San Francisco, December/2015.

3. "Neotectonic Evolution of Anatolia: Comparison of Geodynamical Models and Observations", Poster in Humboldt Kolleg/İstanbul, March/2016.

4. "Geodynamic evolution of the lithosphere beneath the Eastern Anatolia region: Constraints from geodynamic modeling", Poster in EGU/Vienna, April/2016.

Research Activities and Professional Experience

2014-2016 : Project Assistant in TUBITAK (Scientific and Technological Research Council of Turkey), Project name: " Evolution of the lithosphere beneath Eastern and Western Anatolia regions: Insights from numerical modeling", Project coordinator: Assoc. Prof. Oğuz Hakan Göğüş